

Omnidirectional Precoding and Combining Based Synchronization for Millimeter Wave Massive MIMO Systems

Xin Meng, Xiqi Gao, and Xiang-Gen Xia

Abstract

In this paper, we design the precoding matrices at the base station side and the combining matrices at the user terminal side for initial downlink synchronization in millimeter wave massive multiple-input multiple-output systems. First, we demonstrate two basic requirements for the precoding and combining matrices, including that all the entries therein should have constant amplitude under the implementation architecture constraint, and the average transmission power over the total K time slots taking for synchronization should be constant for any spatial direction. Then, we derive the optimal synchronization detector based on generalized likelihood ratio test. By utilizing this detector, we analyze the effect of the precoding and combining matrices to the missed detection probability and the false alarm probability, respectively, and present the corresponding conditions that should be satisfied. It is shown that, both of the precoding and combining matrices should guarantee the perfect omnidirectional coverage at each time slot, i.e., the average transmission power at each time slot is constant for any spatial direction, which is more strict than the second basic requirement mentioned above. We also show that such omnidirectional precoding matrices and omnidirectional combining matrices exist only when both of the number of transmit streams and the number of receive streams are equal to or greater than two. In this case, we propose to utilize Golay complementary pairs and Golay-Hadamard matrices to design the precoding and combining matrices. Simulation results verify the effectiveness of the propose approach.

Index Terms

Millimeter wave (mmWave), massive multiple-input multiple-output (MIMO), synchronization, Golay complementary pair, Golay-Hadamard matrix

X. Meng and X. Q. Gao are with the National Mobile Communications Research Laboratory, Southeast University, Nanjing, 210096, China (e-mail: {xmeng, xqgao}@seu.edu.cn). X.-G. Xia is with the Department of Electrical and Computer Engineering, University of Delaware, Newark, DE 19716, USA (e-mail: xxia@ee.udel.edu).

I. INTRODUCTION

In recent years, utilizing millimeter wave (mmWave) frequency bands from 30 GHz to 300 GHz for cellular wireless communications has received considerable interest from both academia and industry [1]–[5]. Compared with the existing cellular systems operated at carrier frequencies below 6 GHz, mmWave frequencies can offer orders of magnitude more spectrum to support higher data rates. Moreover, the small mmWave wavelengths also make it practical to deploy massive antenna arrays at both of the base station (BS) and user terminal (UT) sides. Hence considerable directional beamforming gains can be provided to compensate for the high isotropic path loss under mmWave frequencies. Therefore, mmWave massive multiple-input multiple-output (MIMO) is considered as one of the major technologies for next generation cellular systems.

Initial synchronization, also referred to as cell search or cell discovery in some literature, is a basic prerequisite to cellular communications. Generally, a BS broadcasts downlink synchronization signals periodically and a UT utilizes these signals to keep time and frequency synchronization with the BS, and then payload data transmission can be established. In the current cellular systems such as long-term evolution (LTE), to ensure cell-wide coverage, a BS usually transmits downlink synchronization signals by using a fixed wide beam pattern [6]. Only after the synchronization has been established and the correct beamforming directions have been obtained, directional narrow beams are used to provide beamforming gains to improve the data rates.

When considering mmWave massive MIMO systems, it was once mentioned that directional narrow beams should also be used in the initial synchronization stage, as well as in the data transmission stage, to overcome the high isotropic path loss. Otherwise, there will be the problem that at one certain distance between a BS and a UT, although a reasonable data rate can be achieved by using directional transmission with beamforming gains, the synchronization cannot be established by using a wide beam pattern with a very low beamforming gain [7], [8]. On the other hand, it is known that different from data signals, the transmitted downlink synchronization signals usually consist of a predefined sequence that is foreknown at both of the BS and UT sides. This may provide additional spreading gains to increase the range of coverage for synchronization signals. For example in LTE, it is a Zadoff-Chu (ZC) sequence of length 63 [9], and the corresponding spreading gain is about 18 dB. Moreover, although

directional transmission increases the range of coverage, it also increases the latency time of synchronization. This is because multiple narrow beams towards different directions have to be used at multiple time slots to guarantee omnidirectional coverage in an average sense, since the correct beamforming directions are not known in the initial synchronization stage.

There have been some studies on mmWave massive MIMO synchronization. The results in [10], [11] showed that omnidirectional transmission is better than random beamforming, and full digital architectures with low resolution has significant benefits in comparison with single-stream analog beamforming. In [12], the authors identified the desired beam pattern in a targeted detectable region and approximated this beam pattern with the proposed designs. The optimal beamforming vectors maximizing the signal-to-noise ratio (SNR) values under different implementation architecture constraints were investigated in [13]. In [14], a per-beam synchronization approach was proposed to moderate the variance of the beam domain channel. In this paper, we mainly consider that when the latency time taking for synchronization is fixed, how to design the precoding matrix at the BS side and the combining matrix at the UT side, to optimize the synchronization performance. Our main contributions are as follows.

- We demonstrate two basic requirements for the precoding matrices at the BS side and the combining matrices at the UT side, including that all the entries therein should have constant amplitude to satisfy the implementation architecture constraint, and the average transmission power over the total K time slots should be constant for any spatial direction, where K corresponds to the total latency time taking for synchronization.
- We derive the optimal synchronization detector based on generalized likelihood ratio test (GLRT). By utilizing this detector, we analyze the effect of the precoding and combining matrices to the missed detection (MD) probability under two special channel models, respectively, including the single-path channel and the independent and identically distributed (i.i.d.) channel, and analyze the effect to the false alarm (FA) probability. We also present the corresponding conditions that the precoding and combining matrices should satisfy. It is shown that, both of the precoding and combining matrices should guarantee the perfect omnidirectional coverage at each time slot, i.e., the average transmission power at each time slot is constant for any spatial direction, which is more strict than the second basic requirement mentioned above.
- We show that to guarantee constant amplitude for all the entries in the precoding and combining matrices, and at the same time guarantee the perfect omnidirectional coverage,

both of the number of transmit streams and the number of receive streams should be equal to or greater than two. In this case, we propose to use Golay complementary pairs and Golay-Hadamard matrices to design the precoding and combining matrices.

Note that omnidirectional coverage for payload data transmission in traditional MIMO systems has been considered in [6], where the authors propose a single-stream solution for the precoding vector, and analyze the system performance in terms of ergodic capacity and bit error rate. In this paper, we mainly focus on initial downlink synchronization in mmWave MIMO systems. We use MD probability and FA probability to evaluate the synchronization performance, and propose a multiple-stream solution for the precoding and combining matrices to guarantee perfect omnidirectional coverage.

The rest of this paper is organized as follows. The system model is presented in Section II, including the synchronization signal model and the channel model. The basic requirements of the precoding and combining matrices are demonstrated in Section III. The effect of the precoding and combining matrices to synchronization performance is analyzed in Section IV. The precoding and combining matrices are designed in Section IV. Numerical results are presented in Section V. Finally, conclusions are drawn in Section VI.

Notations: We use upper-case and lower-case boldfaces to denote matrices and column vectors. \mathbf{I}_M , $\mathbf{1}_M$, and $\mathbf{0}$ denote the $M \times M$ identity matrix, the $M \times 1$ column vector of all ones, and the zero matrix with proper dimensions, respectively. $(\cdot)^*$, $(\cdot)^T$, and $(\cdot)^H$ denote the conjugate, the transpose, and the conjugate transpose, respectively. $\mathbb{E}(\cdot)$ refers to the expectation and $\mathbb{P}(\cdot)$ represents the probability. The Kronecker product of two matrices \mathbf{A} and \mathbf{B} is denoted by $\mathbf{A} \otimes \mathbf{B}$. $[\mathbf{A}]_{m,n}$, $[\mathbf{A}]_{m,:}$, and $[\mathbf{A}]_{:,n}$ denote the (m, n) th element, the m th row vector, and the n th column vector of matrix \mathbf{A} , respectively, and $[\mathbf{a}]_m$ denotes the m th element of vector \mathbf{a} . $\text{diag}(\mathbf{a})$ and $\text{diag}(\mathbf{A})$ denote the diagonal matrix with \mathbf{a} on the main diagonal and the column vector constituted by the main diagonal of \mathbf{A} , respectively. δ_n denotes the Kronecker delta function. $\binom{n}{k} = \frac{n!}{k!(n-k)!}$ denotes the combination number. $\mathcal{A} \cap \mathcal{B} = \emptyset$ means that the intersection of two sets \mathcal{A} and \mathcal{B} is the empty set.

II. SYSTEM MODEL

A. Synchronization Signal Model

Consider initial downlink synchronization in a single cell, where the BS periodically transmits downlink synchronization signals, and a UT detects the presence of these synchronization signals

in received signals to keep temporal synchronization with the BS. This is a typical arrangement in many existing cellular systems such as LTE [9].

We call the time duration that the BS transmits synchronization signals each time as a synchronization time slot. As an example in LTE, a synchronization time slot corresponds to an orthogonal frequency division multiplexing (OFDM) symbol period [9]. The UT is assumed to utilize K consecutive synchronization time slots to synchronize with the BS, where K is an adjustable parameter yielding a tradeoff between the latency time and the success probability of initial synchronization.

At the k th synchronization time slot for $k = 1, 2, \dots, K$, the discrete-time complex baseband signals can be modeled as

$$\mathbf{Y}_k(\tau) = \begin{cases} \mathbf{F}_k^H \mathbf{H}_k \mathbf{W}_k \mathbf{X}_k + \mathbf{F}_k^H \mathbf{Z}_k, & \mathcal{H}_1 : \tau = \tau_0 \\ \mathbf{F}_k^H \mathbf{Z}_k, & \mathcal{H}_0 : \tau \neq \tau_0 \end{cases} \quad (1)$$

where $\mathbf{X}_k \in \mathbb{C}^{N_t \times L}$ denotes the synchronization signal transmitted by the BS at the k th time slot, N_t is the number of transmit streams, i.e., the number of transmit antenna ports, L is the length of \mathbf{X}_k , $\mathbf{W}_k \in \mathbb{C}^{M_t \times N_t}$ denotes the precoding matrix, $\mathbf{H}_k \in \mathbb{C}^{M_r \times M_t}$ denotes the channel matrix, which is assumed to be frequency flat and temporally static in each time slot, but may vary across different time slots, M_r and M_t are the number of UT antennas and the number of BS antennas, respectively, $\mathbf{Z}_k \in \mathbb{C}^{M_r \times L}$ denotes the additive white Gaussian noise (AWGN) matrix with i.i.d. $\mathcal{CN}(0, \nu)$ entries, $\mathbf{F}_k \in \mathbb{C}^{M_r \times N_r}$ denotes the combining matrix, N_r is the number of receive streams, i.e., the number of radio frequency (RF) chains at the UT, $\mathbf{Y}_k(\tau) \in \mathbb{C}^{N_r \times L}$ denotes the signal observed by the UT at timing offset τ after combining. In addition, hypothesis \mathcal{H}_1 represents that timing offset τ is equal to a correct value τ_0 , hence the received signal is aligned with the transmitted synchronization signal, and hypothesis \mathcal{H}_0 means an incorrect τ , therefore the synchronization signal is misaligned or absent [15], [16].

In the previous studies on mmWave massive MIMO synchronization, as well as the protocols of the existing cellular systems, the number of transmit streams for the synchronization signal \mathbf{X}_k was set as $N_t = 1$ [9]–[12]. Take LTE for example, where \mathbf{X}_k is a Zadoff-Chu (ZC) sequence with $N_t = 1$ and $L = 63$ used for the primary synchronization signal [9]. In this paper, the value of N_t is not confined to 1, and the benefits by doing so will be explained in Section V. In addition, without loss of generality, we assume that \mathbf{X}_k satisfies

$$\mathbf{X}_k \mathbf{X}_k^H = \frac{L}{N_t} \mathbf{I}_{N_t} \quad (2)$$

for each k . Otherwise, we can always let \mathbf{X}_k satisfy (2) by properly adjusting the precoding matrix \mathbf{W}_k .

As a remark, it is known that mmWave communications should rely on directional transmitting/receiving beams. At the initial synchronization stage, both of the BS and the UT should find the correct beam directions for payload data transmission. In this paper, we assume that the entire initial synchronization procedure is divided into three steps. At the first step, when a UT is power on or moving to a new cell, it should keep downlink time/frequency synchronization with the BS by utilizing downlink synchronization signals transmitted from this BS. At this step, the target is reliable synchronization, e.g., minimizing the MD probability, in a fixed latency time. At the second step, after synchronized with the BS, the UT needs to find the correct receiving/transmitting beam directions for downlink/uplink transmission. At the last step, the UT transmits uplink synchronization signals with the previously obtained beam directions, and the BS finds the correct receiving/transmitting beam directions for uplink/downlink transmission. In this paper, we focus on the first step.

B. Channel Model

Consider the typical geometric channel model [3], [17], [18]. Both of the BS and UT are assumed to be equipped with a uniform linear array (ULA). Then the channel matrix \mathbf{H}_k in (1) can be expressed as

$$\mathbf{H}_k = \sum_{p=1}^P \alpha_{p,k} \mathbf{u}(\theta_{r,p}) \mathbf{v}^H(\theta_{t,p}) \quad (3)$$

where P denotes the total number of paths, $\alpha_{p,k}$ denotes the complex fading gain of the p th path at the k th synchronization time slot, $\theta_{r,p}$ and $\theta_{t,p}$ denote the arrival and departure angles¹ of the p th path, respectively, and the array response vectors are expressed as

$$\mathbf{u}(\theta_r) = [1, e^{j2\pi\theta_r}, \dots, e^{j2\pi(M_r-1)\theta_r}]^T, \quad 0 \leq \theta_r \leq 1 \quad (4)$$

$$\mathbf{v}(\theta_t) = [1, e^{j2\pi\theta_t}, \dots, e^{j2\pi(M_t-1)\theta_t}]^T, \quad 0 \leq \theta_t \leq 1. \quad (5)$$

¹Here θ represents the virtual angle, also known as spatial frequency. The relation between the virtual angle θ and the physical angle ϑ is $\theta = d \sin \vartheta / \lambda$, where λ denotes the carrier wavelength and d denotes the antenna space of the ULA. A typical value of d is $d = \lambda/2$.

The complex fading gain $\alpha_{p,k}$ of the p th path is assumed to follow complex Gaussian distribution with zero mean and variance β_p , i.e.,

$$\alpha_{p,k} \sim \mathcal{CN}(0, \beta_p). \quad (6)$$

The arrival and departure angles $\theta_{r,p}$ and $\theta_{t,p}$ of each path are assumed to keep constant within these K synchronization time slots since they usually vary slowly compared with the fast fading [19]–[21]. Different paths are assumed to be uncorrelated, and the temporal correlation of each path at the k th and l th synchronization time slots is described as $\psi_{k,l}$, i.e.,

$$\mathbb{E}\{\alpha_{p,k}\alpha_{q,l}^*\} = \begin{cases} \beta_p\psi_{k,l}, & \text{if } p = q \\ 0, & \text{otherwise,} \end{cases} \quad (7)$$

where

$$\psi_{k,k} = 1 \quad (8)$$

and $|\psi_{k,l}| \leq 1$ if $k \neq l$. In addition, the total average gain of all the P paths is assumed to be normalized, i.e.,

$$\sum_{p=1}^P \beta_p = 1. \quad (9)$$

III. BASIC REQUIREMENTS OF PRECODING AND COMBINING MATRICES

A. Implementation Architecture Constraint

In mmWave massive MIMO systems, the precoding and combining are usually implemented in hybrid analog-digital architectures [22]–[24]. Taking precoding for example, the precoding matrix in (1) can be decomposed as $\mathbf{W}_k = \mathbf{W}_{k,\text{RF}}\mathbf{W}_{k,\text{BB}}$, where $\mathbf{W}_{k,\text{RF}} \in \mathbb{C}^{M_t \times N_{\text{RF}}}$ and $\mathbf{W}_{k,\text{BB}} \in \mathbb{C}^{N_{\text{RF}} \times N_t}$ represent the RF and baseband precoding matrices, implemented in the analog and digital domains, respectively, and N_{RF} is the number of RF chains satisfying $M_t \leq N_{\text{RF}} \leq N_t$. In this paper, we assume that both of the precoding and combining are implemented in the analog domain using networks of phase shifters. Therefore all the entries in the precoding and combining matrices should have constant amplitude, i.e.,

$$|[\mathbf{W}_k]_{m,n}| = \frac{1}{\sqrt{M_t}}, \quad \forall m, n, k \quad (10)$$

$$|[\mathbf{F}_k]_{m,n}| = \frac{1}{\sqrt{M_r}}, \quad \forall m, n, k. \quad (11)$$

Note that this analog-only architecture is a more strict constraint than hybrid architectures, and the designed precoding and combining matrices under this architecture can also be easily incorporated in hybrid architectures. Still taking precoding for example, once \mathbf{W}_k has been designed satisfying (10), we can let $\mathbf{W}_{k,\text{RF}} = [\mathbf{W}_k, \mathbf{0}_{M_t \times (N_{\text{RF}} - N_t)}]$ and $\mathbf{W}_{k,\text{BB}} = [\mathbf{I}_{N_t}, \mathbf{0}_{N_t \times (N_{\text{RF}} - N_t)}]^T$, i.e., selecting N_t RF chains from the total N_{RF} RF chains to implement \mathbf{W}_k in hybrid architectures.

B. Omnidirectional Coverage over Total K Time Slots

To overcome the high isotropic path loss in mmWave frequency bands and extend the transmission range, mmWave massive MIMO systems usually rely on highly directional transmission. However, in the initial synchronization stage, neither of the BS and UT knows which departure or arrival direction should be preferred for transmitting or receiving. Therefore, both of them should transmit and receive the synchronization signals omnidirectionally to guarantee reliable coverage.

Assume that there is only one single path in (3) with departure angle θ_t and arrival angle θ_r , i.e., $\mathbf{H}_k = \alpha_k \mathbf{u}(\theta_r) \mathbf{v}^H(\theta_t)$. Recall (1) and under \mathcal{H}_1 , the received signal at the UT side at the k th synchronization time slot without AWGN is $\mathbf{F}_k^H \mathbf{H}_k \mathbf{W}_k \mathbf{X}_k = \alpha_k \mathbf{F}_k^H \mathbf{u}(\theta_r) \mathbf{v}^H(\theta_t) \mathbf{W}_k \mathbf{X}_k$. Then, the sum average signal power over the total K synchronization time slots is

$$\begin{aligned}
 P &= \sum_{k=1}^K P_k = \sum_{k=1}^K \mathbb{E}\{\|\alpha_k \mathbf{F}_k^H \mathbf{u}(\theta_r) \mathbf{v}^H(\theta_t) \mathbf{W}_k \mathbf{X}_k\|_{\mathbb{F}}^2\} \\
 &= \frac{L}{N_t} \sum_{k=1}^K \mathbb{E}\{|\alpha_k|^2\} \mathbf{v}^H(\theta_t) \mathbf{W}_k \mathbf{W}_k^H \mathbf{v}(\theta_t) \mathbf{u}^H(\theta_r) \mathbf{F}_k \mathbf{F}_k^H \mathbf{u}(\theta_r) \\
 &= \frac{L}{N_t} \sum_{k=1}^K \mathbf{v}^H(\theta_t) \mathbf{W}_k \mathbf{W}_k^H \mathbf{v}(\theta_t) \mathbf{u}^H(\theta_r) \mathbf{F}_k \mathbf{F}_k^H \mathbf{u}(\theta_r)
 \end{aligned} \tag{12}$$

where the average is taken over α_k , the third equality is from (2), and the last equality is from (7) and (9). It is expected that the sum average power (12) is constant for any departure angle θ_t and arrival angle θ_r , i.e.,

$$\sum_{k=1}^K \mathbf{v}^H(\theta_t) \mathbf{W}_k \mathbf{W}_k^H \mathbf{v}(\theta_t) \cdot \mathbf{u}^H(\theta_r) \mathbf{F}_k \mathbf{F}_k^H \mathbf{u}(\theta_r) = c, \quad \forall \theta_r, \theta_t \in [0, 1]. \tag{13}$$

To determine the unknown coefficient c therein, we integrate over θ_r and θ_t at both sides of (13). The right hand side is $\int_0^1 \int_0^1 c d\theta_r d\theta_t = c$, and the left hand side can be expressed as

$$\begin{aligned} & \sum_{k=1}^K \int_0^1 \mathbf{u}^H(\theta_r) \mathbf{F}_k \mathbf{F}_k^H \mathbf{u}(\theta_r) d\theta_r \int_0^1 \mathbf{v}^H(\theta_t) \mathbf{W}_k \mathbf{W}_k^H \mathbf{v}(\theta_t) d\theta_t \\ &= \sum_{k=1}^K \text{tr} \left(\mathbf{F}_k \mathbf{F}_k^H \int_0^1 \mathbf{u}(\theta_r) \mathbf{u}^H(\theta_r) d\theta_r \right) \text{tr} \left(\mathbf{W}_k \mathbf{W}_k^H \int_0^1 \mathbf{v}(\theta_t) \mathbf{v}^H(\theta_t) d\theta_t \right) \\ &= \sum_{k=1}^K \text{tr}(\mathbf{F}_k \mathbf{F}_k^H) \text{tr}(\mathbf{W}_k \mathbf{W}_k^H) = K N_r N_t \end{aligned}$$

where the first equality is from the fact that $\text{tr}(\mathbf{A}\mathbf{B}) = \text{tr}(\mathbf{B}\mathbf{A})$, the second equality is because $\int_0^1 \mathbf{u}(\theta_r) \mathbf{u}^H(\theta_r) d\theta_r = \mathbf{I}_{M_r}$ and $\int_0^1 \mathbf{v}(\theta_t) \mathbf{v}^H(\theta_t) d\theta_t = \mathbf{I}_{M_t}$, which can be obtained from (4) and (5) immediately, and the last equality can be obtained from (10) and (11). Therefore, we have $c = K N_r N_t$ and can rewrite (13) as

$$\sum_{k=1}^K \mathbf{u}^H(\theta_r) \mathbf{F}_k \mathbf{F}_k^H \mathbf{u}(\theta_r) \cdot \mathbf{v}^H(\theta_t) \mathbf{W}_k \mathbf{W}_k^H \mathbf{v}(\theta_t) = K N_r N_t, \quad \forall \theta_r, \theta_t \in [0, 1]. \quad (14)$$

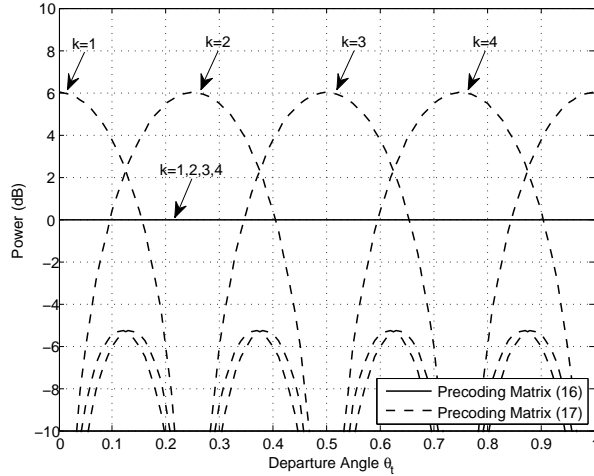


Fig. 1. Comparison of transmit power between two different precoding matrices.

Note that condition (14) implies that the omnidirectional coverage is guaranteed in total K synchronization time slots in an average sense. Hence we call it average omnidirectional coverage, and it does not necessarily require wide beams at both of the BS and UT sides when $K > 1$, since sweeping a narrow beam towards different directions at different time slots can also achieve average omnidirectional coverage. For example, in the case with $M_t = K = 4$ and

$M_r = N_r = N_t = 1$, since there is only one single receive antenna, only precoding needs to be considered. Then (14) becomes

$$\sum_{k=1}^K \mathbf{u}^H(\theta_r) \mathbf{F}_k \mathbf{F}_k^H \mathbf{u}(\theta_r) = KN_t, \quad \forall \theta_t \in [0, 1]. \quad (15)$$

For the following two precoding matrices

$$\mathbf{W}_k^{(1)} = [\mathbf{I}_4]_{:,k} \quad (16)$$

$$\mathbf{W}_k^{(2)} = \frac{1}{2} [1, e^{j\pi k/2}, e^{j\pi k}, e^{j3\pi k/2}]^T, \quad (17)$$

the corresponding transmit power at each departure angle θ_t can be obtained according to $\mathbf{v}^H(\theta_t) \mathbf{W}_k \mathbf{W}_k^H \mathbf{v}(\theta_t)$ for each time slot $k = 1, 2, 3, 4$, and are plotted in Fig. 1. It can be observed that, both precoding matrices (16) and (17) can guarantee average omnidirectional coverage constraint (15) over total 4 synchronization time slots. The difference is that, (16) guarantees omnidirectional coverage in every synchronization time slot, while (17) generates narrow beams toward different directions in different synchronization time slots.

IV. EFFECT OF PRECODING AND COMBINING MATRICES TO SYNCHRONIZATION PERFORMANCE

A. GLRT Based Synchronization Detector

As described in (1), we model the temporal synchronization as a binary hypothesis test problem [15], [16]. Since there are unknown parameters in (1), including the noise variance ν and the effective channel matrix $\mathbf{G}_k \triangleq \mathbf{F}_k^H \mathbf{H}_k \mathbf{W}_k$, we use GLRT to perform synchronization detection [15], [16]. The test statistic under GLRT is defined as

$$T'(\tau) = \ln \frac{\max_{\mathbf{G}, \nu} f(\mathbf{Y}(\tau) | \mathcal{H}_1, \mathbf{G}, \nu)}{\max_{\nu} f(\mathbf{Y}(\tau) | \mathcal{H}_0, \nu)} \underset{\mathcal{H}_0}{\overset{\mathcal{H}_1}{\gtrless}} \gamma' \quad (18)$$

where $\mathbf{Y}(\tau) = [\mathbf{Y}_1(\tau), \mathbf{Y}_2(\tau), \dots, \mathbf{Y}_K(\tau)]$, $\mathbf{G} = [\mathbf{G}_1, \mathbf{G}_2, \dots, \mathbf{G}_K]$, γ' is a threshold value. Then we have the following theorem.

Theorem 1: The test statistic (18) is equivalent to

$$T(\tau) = \frac{\sum_{k=1}^K \text{tr}(\mathbf{Y}_k(\tau) \mathbf{X}_k^H (\mathbf{X}_k \mathbf{X}_k^H)^{-1} \mathbf{X}_k \mathbf{Y}_k^H(\tau) (\mathbf{F}_k^H \mathbf{F}_k)^{-1})}{\sum_{k=1}^K \text{tr}(\mathbf{Y}_k(\tau) \mathbf{Y}_k^H(\tau) (\mathbf{F}_k^H \mathbf{F}_k)^{-1})} \underset{\mathcal{H}_0}{\overset{\mathcal{H}_1}{\gtrless}} \gamma \quad (19)$$

where $\gamma = 1 - \exp\left(-\frac{\gamma'}{KLN_r}\right)$.

Proof: See Appendix A. ■

According to (19), the synchronization detector at the UT is operated as follows. The observed signal $\mathbf{Y}(\tau)$ under timing offset τ is used to evaluate the test statistic $T(\tau)$, which is then compared with the threshold value γ . If $T(\tau)$ is greater than γ , successful synchronization can be claimed. Otherwise, the UT adjusts its timing offset τ , e.g., letting $\tau = \tau + 1$, and re-execute the above procedure until a successful synchronization appears.

The performance of temporal synchronization is typically characterized by the probability of MD given the correct timing offset, versus the probability of FA that occurs if synchronization is declared in error. The MD probability and the FA probability are, respectively, defined as

$$P_{\text{MD}} = \mathbb{P}\{T(\tau) < \gamma | \mathcal{H}_1\} \quad (20)$$

$$P_{\text{FA}} = \mathbb{P}\{T(\tau) > \gamma | \mathcal{H}_0\}. \quad (21)$$

In the following subsections, we will investigate the effect of the precoding and combining matrices to the MD and FA probabilities.

B. MD Probability

In this subsection, we mainly investigate the effect of the recoding and combining matrices to the MD probability. First, we present the following theorem.

Theorem 2: The MD probability (20) can be expressed as

$$P_{\text{MD}} = \mathbb{P}\left\{ \frac{\sum_{k=1}^K \|(L/N_t)^{1/2} \mathbf{F}_k^H \mathbf{H}_k \mathbf{W}_k + \mathbf{Z}_{k,2}\|_{\mathbb{F}}^2}{\sum_{k=1}^K \|\mathbf{Z}_{k,1}\|_{\mathbb{F}}^2} < \frac{\gamma}{1-\gamma} \right\} \quad (22)$$

where $\mathbf{Z}_{k,1} \in \mathbb{C}^{N_r \times (L-N_t)}$ and $\mathbf{Z}_{k,2} \in \mathbb{C}^{N_r \times N_t}$ are both with i.i.d. $\mathcal{CN}(0, \nu)$ entries and they are independent of each other.

Proof: See Appendix B. ■

By letting

$$\mathbf{g} = \text{vec}\{[\mathbf{F}_1^H \mathbf{H}_1 \mathbf{W}_1, \dots, \mathbf{F}_K^H \mathbf{H}_K \mathbf{W}_K]\} \quad (23)$$

$$\mathbf{z}_1 = \text{vec}\{[\mathbf{Z}_{1,1}, \mathbf{Z}_{2,1}, \dots, \mathbf{Z}_{K,1}]\}$$

$$\mathbf{z}_2 = \text{vec}\{[\mathbf{Z}_{1,2}, \mathbf{Z}_{2,2}, \dots, \mathbf{Z}_{K,2}]\},$$

we can express (22) as

$$P_{\text{MD}} = \mathbb{P}\left\{ \frac{((L/N_t)^{1/2} \mathbf{g} + \mathbf{z}_2)^H ((L/N_t)^{1/2} \mathbf{g} + \mathbf{z}_2)}{\mathbf{z}_1^H \mathbf{z}_1} < \frac{\gamma}{1-\gamma} \right\} \quad (24)$$

where $\mathbf{z}_1 \sim \mathcal{CN}(\mathbf{0}, \nu \mathbf{I}_{KN_r(L-N_t)})$ and $\mathbf{z}_2 \sim \mathcal{CN}(\mathbf{0}, \nu \mathbf{I}_{KN_r N_t})$. According to (3), (6), and (23), we have $\mathbf{g} \sim \mathcal{CN}(\mathbf{0}, \mathbf{R})$ where the covariance matrix can be expressed as

$$\mathbf{R} = \mathbb{E}\{\mathbf{g}\mathbf{g}^H\} = \begin{bmatrix} \mathbf{R}_{1,1} & \mathbf{R}_{1,2} & \cdots & \mathbf{R}_{1,K} \\ \mathbf{R}_{2,1} & \mathbf{R}_{2,2} & \cdots & \mathbf{R}_{2,K} \\ \vdots & \vdots & \ddots & \vdots \\ \mathbf{R}_{K,1} & \mathbf{R}_{K,2} & \cdots & \mathbf{R}_{K,K} \end{bmatrix}. \quad (25)$$

The (k, l) th subblock in (25) is defined as

$$\begin{aligned} \mathbf{R}_{k,l} &= \mathbb{E}\{\text{vec}(\mathbf{F}_k^H \mathbf{H}_k \mathbf{W}_k) (\text{vec}(\mathbf{F}_l^H \mathbf{H}_l \mathbf{W}_l))^H\} \\ &= (\mathbf{W}_k^T \otimes \mathbf{F}_k^H) \mathbb{E}\{\text{vec}(\mathbf{H}_k) (\text{vec}(\mathbf{H}_l))^H\} (\mathbf{W}_l^* \otimes \mathbf{F}_l) \end{aligned} \quad (26)$$

where the last equality is with the fact that $\text{vec}(\mathbf{ABC}) = (\mathbf{C}^T \otimes \mathbf{A})\text{vec}(\mathbf{B})$. The middle term in (26) can be further expressed as

$$\begin{aligned} \mathbb{E}\{\text{vec}(\mathbf{H}_k) (\text{vec}(\mathbf{H}_l))^H\} &= \mathbb{E}\left\{ \left(\sum_{p=1}^P \alpha_{p,k} \mathbf{v}^*(\theta_{t,p}) \otimes \mathbf{u}(\theta_{r,p}) \right) \left(\sum_{p=1}^P \alpha_{p,l} \mathbf{v}^*(\theta_{t,p}) \otimes \mathbf{u}(\theta_{r,p}) \right)^H \right\} \\ &= \psi_{k,l} \sum_{p=1}^P \beta_p (\mathbf{v}^*(\theta_{t,p}) \otimes \mathbf{u}(\theta_{r,p})) (\mathbf{v}^T(\theta_{t,p}) \otimes \mathbf{u}^H(\theta_{r,p})) \end{aligned} \quad (27)$$

where the first equality is from (3) and the last equality is from (7).

From (24), (25), and (26), it can be observed that the precoding and combining matrices over total K synchronization time slots $\{\mathbf{W}_k, \mathbf{F}_k\}_{k=1}^K$ mainly affect the covariance matrix \mathbf{R} of the effective channel vector \mathbf{g} , thereby affecting the MD probability P_{MD} . To further quantify this effect, we need to derive an exact expression for (24). Before proceeding, we present the following useful lemma.

Lemma 1: Consider two random variables $X = \sum_{m=1}^M |x_m|^2$ and $Y = \sum_{n=1}^N |y_n|^2$ with independently distributed entries $x_m \sim \mathcal{CN}(0, \lambda_m)$ and $y_n \sim \mathcal{CN}(0, \sigma_n)$. Then the probability $\mathbb{P}\{\frac{X}{Y} < t\}$ can be approximated by

$$\mathbb{P}\left\{\frac{X}{Y} < t\right\} \approx t^M \prod_{m=1}^M \frac{1}{\lambda_m} \sum_{l_1+l_2+\dots+l_N=M} \prod_{n=1}^N \sigma_n^{l_n} \quad (28)$$

when t is small.

Proof: See Appendix C. ■

Note that the M components x_1, x_2, \dots, x_M in X , as well as the N components y_1, y_2, \dots, y_N in Y , may have different variances. Therefore, X and Y do not follow the standard Chi-squared

distribution. Hence, X/Y does not follow the traditional F-distribution. The above lemma is then used to establish the following theorem.

Theorem 3: Let r and $\{\lambda_m\}_{m=1}^r$ denote the rank and the non-zero eigenvalues of \mathbf{R} , respectively. Then the MD probability (24) can be asymptotically expressed as

$$P_{\text{MD}} \approx \left(\frac{N_t \nu \gamma}{L(1-\gamma)} \right)^r \binom{KLN_r - 1}{r} \prod_{m=1}^r \lambda_m^{-1} \quad (29)$$

when γ is small, where $\binom{n}{k} = \frac{n!}{k!(n-k)!}$ denotes the combination number.

Proof: It can be obtained from Lemma 1 immediately. ■

The asymptotic result (29) in Theorem 1 presents a simple and useful tool to analyze the effect of the precoding and combining matrices to the MD probability. From (29), it can be observed that P_{MD} is mainly affected by the rank r and the non-zero eigenvalues $\{\lambda_m\}_{m=1}^r$ of \mathbf{R} . If we regard P_{MD} as a function of the signal-to-noise ratio (SNR) value $1/\nu$, the slope of the curve in the high-SNR regime as in (29) will be determined by r , and the horizontal shift of the curve will be determined by $\prod_{m=1}^r \lambda_m^{-1}$. This is similar to the concepts of diversity and coding gains of traditional space-time block codes (STBCs), where a good STBC design should first maximize the diversity gain, and then maximize the coding gain [25]. Here, the same with the design criteria for STBC, to minimize the asymptotic P_{MD} (29), it is required that the rank r of \mathbf{R} should be maximized first, and then the product of the non-zero eigenvalues $\prod_{m=1}^r \lambda_m$ of \mathbf{R} should be maximized.

However, from (25) and (26) one can see that the rank r and the non-zero eigenvalues $\{\lambda_m\}_{m=1}^r$ of \mathbf{R} are determined not only by the precoding and combining matrices $\{\mathbf{W}_k, \mathbf{F}_k\}_{k=1}^K$, but also by the channel covariance matrix $\mathbb{E}\{\text{vec}(\mathbf{H}_k)\text{vec}(\mathbf{H}_l)^H\}$. This covariance matrix usually depends on the transmission scenario and the characteristics of the terrain, and cannot be foreknown in the initial synchronization stage. Therefore, we consider two typical models, including the single-path channel and the i.i.d. channel. These two models represent two extreme transmission scenarios, where the former is with a single sparse path while the latter is with sufficiently rich paths. Note that these two models are mainly used to simplify the theory analysis, and in numerical simulations we will also use more realistic channel models.

1) The single-path channel: In this case, there is only $P = 1$ path in (3), and then (27) becomes

$$\mathbb{E}\{\text{vec}(\mathbf{H}_k)\text{vec}(\mathbf{H}_l)^H\} = \psi_{k,l}(\mathbf{v}^*(\theta_t) \otimes \mathbf{u}(\theta_r))(\mathbf{v}^T(\theta_t) \otimes \mathbf{u}^H(\theta_r)) \quad (30)$$

where we have utilized (9) and omitted the path index p for notational simplicity. Substituting (30) into (26) yields

$$\mathbf{R}_{k,l} = \psi_{k,l} \underbrace{(\mathbf{W}_k^T \mathbf{v}^*(\theta_t) \otimes \mathbf{F}_k^H \mathbf{u}(\theta_r))}_{\mathbf{a}_k} \underbrace{(\mathbf{v}^T(\theta_t) \mathbf{W}_l^* \otimes \mathbf{u}^H(\theta_r) \mathbf{F}_l)}_{\mathbf{a}_l^H}. \quad (31)$$

Let

$$\mathbf{A} = \begin{bmatrix} \mathbf{a}_1 & \mathbf{0} & \cdots & \mathbf{0} \\ \mathbf{0} & \mathbf{a}_2 & \cdots & \mathbf{0} \\ \vdots & \vdots & \ddots & \vdots \\ \mathbf{0} & \mathbf{0} & \cdots & \mathbf{a}_K \end{bmatrix}$$

and $[\Psi]_{k,l} = \psi_{k,l}$. Then with (31), we can express (25) as

$$\mathbf{R} = \mathbf{A} \Psi \mathbf{A}^H. \quad (32)$$

Assume Ψ is of full rank K . According to the property that two matrices $\mathbf{X}\mathbf{Y}$ and $\mathbf{Y}\mathbf{X}$ have the same rank and non-zero eigenvalues when \mathbf{X} is invertible, we know that the rank and the non-zero eigenvalues of \mathbf{R} in (32) are identical to those of

$$\tilde{\mathbf{R}} = \Psi \mathbf{A}^H \mathbf{A} = \Psi \cdot \text{diag}\{\mathbf{a}_1^H \mathbf{a}_1, \mathbf{a}_2^H \mathbf{a}_2, \dots, \mathbf{a}_K^H \mathbf{a}_K\}. \quad (33)$$

With (31) we know that

$$\begin{aligned} \mathbf{a}_k^H \mathbf{a}_k &= (\mathbf{v}^T(\theta_t) \mathbf{W}_k^* \otimes \mathbf{u}^H(\theta_r) \mathbf{F}_k) (\mathbf{W}_k^T \mathbf{v}^*(\theta_t) \otimes \mathbf{F}_k^H \mathbf{u}(\theta_r)) \\ &= \mathbf{v}^T(\theta_t) \mathbf{W}_k^* \mathbf{W}_k^T \mathbf{v}^*(\theta_t) \otimes \mathbf{u}^H(\theta_r) \mathbf{F}_k \mathbf{F}_k^H \mathbf{u}(\theta_r) \\ &= \mathbf{v}^H(\theta_t) \mathbf{W}_k \mathbf{W}_k^H \mathbf{v}(\theta_t) \cdot \mathbf{u}^H(\theta_r) \mathbf{F}_k \mathbf{F}_k^H \mathbf{u}(\theta_r), \end{aligned} \quad (34)$$

where the second equality is because $(\mathbf{A} \otimes \mathbf{B})(\mathbf{C} \otimes \mathbf{D}) = \mathbf{AC} \otimes \mathbf{BD}$, and the last equality is because $a \otimes b = ab$ for two scalars a and b , and $\mathbf{v}^T(\theta_t) \mathbf{W}_k^* \mathbf{W}_k^T \mathbf{v}^*(\theta_t)$ is equal to its transpose $\mathbf{v}^H(\theta_t) \mathbf{W}_k \mathbf{W}_k^H \mathbf{v}(\theta_t)$. With (34) and recall (14), it should be satisfied that

$$\sum_{k=1}^K \mathbf{a}_k^H \mathbf{a}_k = K N_r N_t. \quad (35)$$

As mentioned before, to minimize the asymptotic MD probability in (29), the rank and the product of the non-zero eigenvalues of \mathbf{R} in (32), i.e., the rank and the product of the non-zero eigenvalues of $\tilde{\mathbf{R}}$ in (33), should be maximized. It is not hard to see that, for an arbitrary Ψ , the rank of $\tilde{\mathbf{R}}$ can be maximized if and only if the $K \times K$ diagonal matrix

$\text{diag}\{\mathbf{a}_1^H \mathbf{a}_1, \mathbf{a}_2^H \mathbf{a}_2, \dots, \mathbf{a}_K^H \mathbf{a}_K\}$ is of full rank K . In addition, when Ψ is of full rank K , the product of the non-zero eigenvalues, i.e., the determinant of $\tilde{\mathbf{R}}$ follows

$$\begin{aligned} \det(\tilde{\mathbf{R}}) &= \det(\Psi) \det(\text{diag}\{\mathbf{a}_1^H \mathbf{a}_1, \mathbf{a}_2^H \mathbf{a}_2, \dots, \mathbf{a}_K^H \mathbf{a}_K\}) \\ &= \det(\Psi) \prod_{k=1}^K \mathbf{a}_k^H \mathbf{a}_k \leq \det(\Psi) \left(\frac{1}{K} \sum_{k=1}^K \mathbf{a}_k^H \mathbf{a}_k \right)^K = \det(\Psi) (N_r N_t)^K \end{aligned}$$

where the last equality is with (35), and the equality holds if and only if all $\mathbf{a}_k^H \mathbf{a}_k$ have equal values, i.e.,

$$\mathbf{v}^H(\theta_t) \mathbf{W}_k \mathbf{W}_k^H \mathbf{v}(\theta_t) \cdot \mathbf{u}^H(\theta_r) \mathbf{F}_k \mathbf{F}_k^H \mathbf{u}(\theta_r) = N_r N_t, \quad \forall \theta_r, \theta_t \in [0, 1] \text{ and } \forall k. \quad (36)$$

Moreover, in (36) we assume $\mathbf{v}^H(\theta_t) \mathbf{W}_k \mathbf{W}_k^H \mathbf{v}(\theta_t) = c$ and integrate over θ_t on the interval $[0, 1]$ at both sides. The right hand side is $\int_0^1 c d\theta_t = c$, and the left hand side is

$$\int_0^1 \mathbf{v}^H(\theta_t) \mathbf{W}_k \mathbf{W}_k^H \mathbf{v}(\theta_t) d\theta_t = \text{tr} \left(\mathbf{W}_k \mathbf{W}_k^H \int_0^1 \mathbf{v}(\theta_t) \mathbf{v}^H(\theta_t) d\theta_t \right) = \text{tr}(\mathbf{W}_k \mathbf{W}_k^H) = N_t$$

where the first equality is with the fact that $\text{tr}(\mathbf{AB}) = \text{tr}(\mathbf{BA})$, the second equality is because $\int_0^1 \mathbf{v}(\theta_t) \mathbf{v}^H(\theta_t) d\theta_t = \mathbf{I}_{M_t}$, which can be obtained from (5) immediately, and the last equality can be obtained from (11). Therefore, we have $c = N_t$ and can rewrite (36) as

$$\mathbf{v}^H(\theta_t) \mathbf{W}_k \mathbf{W}_k^H \mathbf{v}(\theta_t) = N_t, \quad \forall \theta_t \in [0, 1] \text{ and } \forall k \quad (37)$$

$$\mathbf{u}^H(\theta_r) \mathbf{F}_k \mathbf{F}_k^H \mathbf{u}(\theta_r) = N_r, \quad \forall \theta_r \in [0, 1] \text{ and } \forall k. \quad (38)$$

One can observe that, conditions (37) and (38) are more strict than (14), since (14) implies that omnidirectional coverage is guaranteed over K synchronization time slots, while (37) and (38) mean that omnidirectional coverage should be guaranteed at every time slot. This implies that omnidirectional transmission is superior to directional narrow beams. In [6], the authors take cyclic delay diversity (CDD) for example. They illustrate that omnidirectional transmission is superior to directional narrow beams when considering payload data transmission. Here, we show that omnidirectional transmission is still superior to directional narrow beams when considering synchronization signals.

2) *The i.i.d. channel:* In this case, there are sufficiently large number of paths in (3), and we have

$$\mathbb{E}\{\text{vec}(\mathbf{H}_k) (\text{vec}(\mathbf{H}_l))^H\} = \psi_{k,l} \mathbf{I}_{M_r M_t}. \quad (39)$$

Substituting (39) into (26) yields

$$\mathbf{R}_{k,l} = \psi_{k,l}(\mathbf{W}_k^T \otimes \mathbf{F}_k^H)(\mathbf{W}_l^* \otimes \mathbf{F}_l) = \psi_{k,l}\mathbf{W}_k^T\mathbf{W}_l^* \otimes \mathbf{F}_k^H\mathbf{F}_l. \quad (40)$$

With (40), we can express (25) as

$$\mathbf{R} = \begin{bmatrix} \psi_{1,1}\mathbf{W}_1^T\mathbf{W}_1^* \otimes \mathbf{F}_1^H\mathbf{F}_1 & \psi_{1,2}\mathbf{W}_1^T\mathbf{W}_2^* \otimes \mathbf{F}_1^H\mathbf{F}_2 & \cdots & \psi_{1,K}\mathbf{W}_1^T\mathbf{W}_K^* \otimes \mathbf{F}_1^H\mathbf{F}_K \\ \psi_{2,1}\mathbf{W}_2^T\mathbf{W}_1^* \otimes \mathbf{F}_2^H\mathbf{F}_1 & \psi_{2,2}\mathbf{W}_2^T\mathbf{W}_2^* \otimes \mathbf{F}_2^H\mathbf{F}_2 & \cdots & \psi_{2,K}\mathbf{W}_2^T\mathbf{W}_K^* \otimes \mathbf{F}_2^H\mathbf{F}_K \\ \vdots & \vdots & \ddots & \vdots \\ \psi_{K,1}\mathbf{W}_K^T\mathbf{W}_1^* \otimes \mathbf{F}_K^H\mathbf{F}_1 & \psi_{K,2}\mathbf{W}_K^T\mathbf{W}_2^* \otimes \mathbf{F}_K^H\mathbf{F}_2 & \cdots & \psi_{K,K}\mathbf{W}_K^T\mathbf{W}_K^* \otimes \mathbf{F}_K^H\mathbf{F}_K \end{bmatrix}. \quad (41)$$

As explained before, to minimize the asymptotic MD probability in (29), the rank and the product of the non-zero eigenvalues of \mathbf{R} in (41) should be maximized. Note that the trace of the $KN_rN_t \times KN_rN_t$ matrix \mathbf{R} in (41) is

$$\text{tr}(\mathbf{R}) = \sum_{k=1}^K \text{tr}(\psi_{k,k}\mathbf{W}_k^T\mathbf{W}_k^* \otimes \mathbf{F}_k^H\mathbf{F}_k) = \sum_{k=1}^K \text{tr}(\mathbf{W}_k^H\mathbf{W}_k)\text{tr}(\mathbf{F}_k^H\mathbf{F}_k) = KN_rN_t$$

where the second equality is with (8) and the property that $\text{tr}(\mathbf{A} \otimes \mathbf{B}) = \text{tr}(\mathbf{A})\text{tr}(\mathbf{B})$ and $\text{tr}(\mathbf{A}) = \text{tr}(\mathbf{A}^T)$, and the last equality can be obtained from (10) and (11) immediately. Therefore, the rank of \mathbf{R} can be maximized to be KN_rN_t and the product of non-zero eigenvalues \mathbf{R} , i.e., the determinant when \mathbf{R} is with full rank, can be maximized to be $\det(\mathbf{R}) \leq (\frac{1}{KN_rN_t}\text{tr}(\mathbf{R}))^{KN_rN_t} = 1$ if and only if $\mathbf{R} = \mathbf{I}_{KN_rN_t}$. For an arbitrary channel temporal correlation matrix Ψ with $[\Psi]_{k,l} = \psi_{k,l}$ in (41), the equality $\mathbf{R} = \mathbf{I}_{KN_rN_t}$ holds if and only if

$$\mathbf{W}_k^T\mathbf{W}_l^* \otimes \mathbf{F}_k^H\mathbf{F}_l = \begin{cases} \mathbf{I}_{N_rN_t}, & \text{if } k = l \\ \mathbf{0}, & \text{otherwise.} \end{cases}$$

This implies that at each synchronization time slot, both of the precoding and combining matrices should be unitary, i.e.,

$$\mathbf{W}_k^H\mathbf{W}_k = \mathbf{I}_{N_t}, \quad \forall k \quad (42)$$

$$\mathbf{F}_k^H\mathbf{F}_k = \mathbf{I}_{N_r}, \quad \forall k. \quad (43)$$

Moreover, at two different synchronization time slots, either the precoding matrices or the combining matrices at these two time slots should be orthogonal to each other, i.e.,

$$\mathbf{W}_k^H\mathbf{W}_l = \mathbf{0} \text{ or } \mathbf{F}_k^H\mathbf{F}_l = \mathbf{0}, \quad \forall k \neq l. \quad (44)$$

C. FA Probability

In this subsection, we mainly investigate the effect of the recoding and combining matrices to the FA probability. First, we present the following theorem.

Theorem 4: The FA probability (21) can be expressed as

$$P_{\text{FA}} = \mathbb{P} \left\{ \frac{\sum_{k=1}^K \|\mathbf{Z}_{k,2}\|_{\text{F}}^2}{\sum_{k=1}^K \|\mathbf{Z}_{k,1}\|_{\text{F}}^2} > \frac{\gamma}{1-\gamma} \right\} \quad (45)$$

where $\mathbf{Z}_{k,1} \in \mathbb{C}^{N_r \times (L-N_t)}$ and $\mathbf{Z}_{k,2} \in \mathbb{C}^{N_r \times N_t}$ are both with i.i.d. $\mathcal{CN}(0, \nu)$ entries and they are independent of each other.

Proof: See Appendix B. ■

It can be observed that neither the precoding matrix nor the combining matrix affects the FA probability (45). Moreover, note that the left hand side in $\mathbb{P}(\cdot)$ in (45) follows the standard F-distribution. Therefore, according to the cumulative distribution function (CDF) of F-distribution, a closed-form expression of (45) can be expressed as [26]

$$P_{\text{FA}} = (1-\gamma)^{KL N_r - 1} \sum_{m=0}^{KL N_r - 1} \binom{KL N_r - 1}{m} \left(\frac{\gamma}{1-\gamma} \right)^m. \quad (46)$$

As a conclusion of this section, we have analyzed the effect of the precoding and combining matrices $\{\mathbf{W}_k, \mathbf{F}_k\}_{k=1}^K$ to the synchronization performance. It is shown that $\{\mathbf{W}_k, \mathbf{F}_k\}_{k=1}^K$ should satisfy (37) and (38) to minimize the asymptotic MD probability under the single-path channel, and satisfy (42), (43), and (44) to minimize the asymptotic MD probability under the i.i.d. channel. Moreover, it is shown that $\{\mathbf{W}_k, \mathbf{F}_k\}_{k=1}^K$ do not affect the FA probability.

V. DESIGN OF PRECODING AND COMBINING MATRICES

In Section III, it is shown that the precoding and combining matrices $\{\mathbf{W}_k, \mathbf{F}_k\}_{k=1}^K$ should satisfy conditions (10), (11), and (14) to guarantee the requirements of constant amplitude for all the entries therein and omnidirectional coverage over total K synchronization time slots. In Section IV, it is shown that $\{\mathbf{W}_k, \mathbf{F}_k\}_{k=1}^K$ should satisfy conditions (37), (38), (42), (43), and (44) to minimize the asymptotic MD probability under the single-path channel and the i.i.d. channel. Note that (14) can be satisfied automatically as long as (37) and (38) have been satisfied, hence it can be ignored. In this section, we will investigate how to design $\{\mathbf{W}_k, \mathbf{F}_k\}_{k=1}^K$ to satisfy conditions (10), (11), (37), (38), (42), (43), and (44) simultaneously.

First, to simplify the problem, we consider the case with $K = 1$, then condition (44) can be ignored temporarily. Since conditions (10), (37), and (42) are similar to (11), (38), and (43),

respectively, the design of the precoding matrix and the design of the combining matrix will also be similar. Therefore in the following contents, we mainly take precoding for example to describe the design procedure. We rewrite conditions (10), (37), and (42) as

$$[\mathbf{W}]_{m,n} = \frac{1}{\sqrt{M}}, \quad \forall m, n \quad (47)$$

$$\mathbf{v}^H(\theta)\mathbf{W}\mathbf{W}^H\mathbf{v}(\theta) = 1, \quad \forall \theta \in [0, 1] \quad (48)$$

$$\mathbf{W}^H\mathbf{W} = \mathbf{I}_N \quad (49)$$

where we have omitted the subscripts k and t for notational simplicity. We need to design matrix $\mathbf{W} \in \mathbb{C}^{M \times N}$ to satisfy (47), (48), and (49) simultaneously.

Letting $\mathbf{W} = [\mathbf{w}_1, \mathbf{w}_2, \dots, \mathbf{w}_N]$ and $\mathbf{w}_n = [w_{1,n}, w_{2,n}, \dots, w_{M,n}]^T$, we can rewrite (48) as

$$\mathbf{v}^H(\theta)\mathbf{W}\mathbf{W}^H\mathbf{v}(\theta) = \sum_{n=1}^N \left| \sum_{m=1}^M w_{m,n} e^{j2\pi(m-1)\theta} \right|^2 = \sum_{l=-M+1}^{M-1} \sum_{n=1}^N r_{l,n} e^{j2\pi l\theta} \quad (50)$$

where

$$r_{l,n} = \begin{cases} \sum_{m=1}^M w_m w_{m+l}^*, & l = 0, 1, \dots, M-1 \\ r_{-l,n}^*, & l = -M+1, \dots, -1 \end{cases}$$

represents the aperiodic autocorrelation function of \mathbf{w}_n , if we regard vector \mathbf{w}_n as a sequence of length M . Substituting (50) into (48) yields

$$\sum_{l=-M+1}^{M-1} \sum_{n=1}^N r_{l,n} e^{j2\pi l\theta} = 1, \quad \forall \theta \in [0, 1]. \quad (51)$$

According to the property of Fourier transform, we know that (51) holds if and only if

$$\sum_{n=1}^N r_{l,n} = \delta_l, \quad (52)$$

i.e., the N respective aperiodic autocorrelation functions of $\{\mathbf{w}_n\}_{n=1}^N$ sum to a Kronecker delta function. We need to design such N vectors $\{\mathbf{w}_n\}_{n=1}^N$ satisfying (52), (47), and (49) simultaneously.

When $N = 1$, i.e., there is only one vector \mathbf{w} and we have omitted the subscript n for notational simplicity, condition (52) implies that the aperiodic autocorrelation function of \mathbf{w} is a Kronecker delta function. However, it is known that the aperiodic autocorrelation function of \mathbf{w} is a Kronecker delta function if and only if there is only one non-zero entry in \mathbf{w} . This implies that condition (47) cannot be satisfied simultaneously since it requires constant amplitude for

all the M entries in \mathbf{w} . Therefore, when employing single-stream precoding at the BS side or single-stream combining at the UT side, it is impossible to generate perfect omnidirectional beam while guaranteeing constant amplitude for all the entries in the precoding or combining matrix. In our previous studies [27], [28], we proposed to use ZC sequences as the precoding vector. Note that this approach can only guarantee equal transmission power in discrete angles, i.e., quasi-omnidirectional.

However, when $N = 2$, the situation begins to change. We will show that in this case, conditions (47), (48), and (49) can be satisfied simultaneously. Before proceeding, we introduce the Golay complementary pair, which was first proposed by M. Golay in the context of infrared spectrometry [29]. A Golay complementary pair consists of two binary sequences, i.e., vectors, with the same length and satisfying the complementary property that the respective aperiodic autocorrelation functions of these two vectors sum to a Kronecker delta function [30]. There are many approaches to construct Golay complementary pairs, including direct constructions and recursive constructions [30]–[32]. Here, we introduce the Golay-Rudin-Shapiro recursion construction [30], where the two vectors $\mathbf{p}_{M,1}$ and $\mathbf{p}_{M,2}$ of length M are recursively constructed with the two vectors $\mathbf{p}_{M/2,1}$ and $\mathbf{p}_{M/2,2}$ of length $M/2$ as

$$\mathbf{p}_{M,1} = \begin{bmatrix} \mathbf{p}_{M/2,1} \\ \mathbf{p}_{M/2,2} \end{bmatrix}, \quad \mathbf{p}_{M,2} = \begin{bmatrix} \mathbf{p}_{M/2,1} \\ -\mathbf{p}_{M/2,2} \end{bmatrix} \quad (53)$$

with initial vectors $\mathbf{p}_{1,1} = \mathbf{p}_{1,2} = [1]$. Moreover, it is shown that the respective aperiodic autocorrelation functions of $\mathbf{p}_{M,1}$ and $\mathbf{p}_{M,2}$ constructed with (53) sum to a Kronecker delta function [30].

With the Golay complementary pair, the design is straightforward as long as we let $\mathbf{W} = \frac{1}{\sqrt{M}}[\mathbf{p}_{M,1}, \mathbf{p}_{M,2}]$. Since both $\mathbf{p}_{M,1}$ and $\mathbf{p}_{M,2}$ are binary vectors, condition (47) can be satisfied. The complementary property of $\mathbf{p}_{M,1}$ and $\mathbf{p}_{M,2}$ lets condition (51), i.e., (48) be satisfied. Moreover, $\mathbf{p}_{M,1}$ and $\mathbf{p}_{M,2}$ are also orthogonal to each other, hence condition (49) can be satisfied.

Then consider the case with $N > 2$ and N is even, we can use the Golay-Hadamard matrix [33], a generalization of the Golay complementary pair, for the design. An $M \times M$ Golay-Hadamard matrix \mathbf{P}_M can be recursively constructed as

$$\mathbf{P}_M = \begin{bmatrix} \mathbf{P}_{M/2} & \mathbf{P}_{M/2} \\ \tilde{\mathbf{P}}_{M/2} & -\tilde{\mathbf{P}}_{M/2} \end{bmatrix}, \quad \tilde{\mathbf{P}}_M = \begin{bmatrix} \mathbf{P}_{M/2} & \mathbf{P}_{M/2} \\ -\tilde{\mathbf{P}}_{M/2} & \tilde{\mathbf{P}}_{M/2} \end{bmatrix} \quad (54)$$

with initial matrices $\mathbf{P}_1 = \tilde{\mathbf{P}}_1 = [1]$. For a Golay-Hadamard matrix \mathbf{P}_M constructed from (54), it can be proved that the n th column and the $(M/2 + n)$ th column of \mathbf{P}_M constitute a Golay complementary pair for $n = 1, 2, \dots, M/2$ [33]. By using this complementary property, the design of matrix \mathbf{W} can be completed by selecting the n_l th column and the corresponding $(M/2 + n_l)$ th column of \mathbf{P}_M for $l = 1, 2, \dots, N/2$, totally N columns, as the columns of \mathbf{W} . In mathematical expression we have

$$\mathbf{W} = \frac{1}{\sqrt{M}} \left[[\mathbf{P}_M]_{:,n_1}, [\mathbf{P}_M]_{:,n_1+M/2}, \dots, [\mathbf{P}_M]_{:,n_{N/2}}, [\mathbf{P}_M]_{:,n_{N/2}+M/2} \right]$$

where $n_1, n_2, \dots, n_{N/2} \in \{1, 2, \dots, M/2\}$ need to be different from each other. Obviously, with the above constructed \mathbf{W} , conditions (47) and (48) can be satisfied. In addition, since \mathbf{P}_M itself is a unitary matrix, all the N columns of \mathbf{W} will be orthogonal to each other. Hence condition (49) can also be satisfied.

Finally, we consider the general case with $K \geq 1$ and present the design of the precoding and combining matrices $\{\mathbf{W}_k, \mathbf{F}_k\}_{k=1}^K$. Note that each \mathbf{W}_k is of size $M_t \times N_t$ and each \mathbf{F}_k is of size $M_r \times N_r$. Let both M_t and M_r be an integer power of 2, and both N_t and N_r be an integer multiple of 2. Then \mathbf{W}_k and \mathbf{F}_k can be constructed as

$$\mathbf{W}_k = \frac{1}{\sqrt{M_t}} \left[[\mathbf{P}_{M_t}]_{:,n_{t,k,1}}, [\mathbf{P}_{M_t}]_{:,n_{t,k,1}+M_t/2}, \dots, [\mathbf{P}_{M_t}]_{:,n_{t,k,N_t/2}}, [\mathbf{P}_{M_t}]_{:,n_{t,k,N_t/2}+M_t/2} \right] \quad (55)$$

$$\mathbf{F}_k = \frac{1}{\sqrt{M_r}} \left[[\mathbf{P}_{M_r}]_{:,n_{r,k,1}}, [\mathbf{P}_{M_r}]_{:,n_{r,k,1}+M_r/2}, \dots, [\mathbf{P}_{M_r}]_{:,n_{r,k,N_r/2}}, [\mathbf{P}_{M_r}]_{:,n_{r,k,N_r/2}+M_r/2} \right] \quad (56)$$

where both \mathbf{P}_{M_t} and \mathbf{P}_{M_r} are Golay-Hadamard matrices constructed according to (54), for each k , $n_{t,k,1}, n_{t,k,2}, \dots, n_{t,k,N_t/2} \in \{1, 2, \dots, M_t/2\}$ need to be different from each other, and $n_{r,k,1}, n_{r,k,2}, \dots, n_{r,k,N_r/2} \in \{1, 2, \dots, M_r/2\}$ need to be different from each other. In addition, to satisfy condition (44), for each $k \neq l$, it should be satisfied that $\{n_{t,k,1}, n_{t,k,2}, \dots, n_{t,k,N_t/2}\} \cap \{n_{t,l,1}, n_{t,l,2}, \dots, n_{t,l,N_t/2}\} = \emptyset$ or $\{n_{r,k,1}, n_{r,k,2}, \dots, n_{r,k,N_r/2}\} \cap \{n_{r,l,1}, n_{r,l,2}, \dots, n_{r,l,N_r/2}\} = \emptyset$.

VI. NUMERICAL RESULTS

In this section, we present numerical simulations to evaluate the performance of mmWave massive MIMO synchronization with the proposed omnidirectional precoding and combining approach. The BS has $M_t = 64$ antennas and the UT has $M_r = 16$ antennas. The number of channel paths in (3) is set as $P = 1$ or $P = 4$. For both of these two cases, the arrival and departure angles $\theta_{r,p}$ and $\theta_{t,p}$ of each path in (3) randomly take values in $[0, 1]$, and the average gain of each path in (6) is $\beta_p = 1/P$. The temporal correlation coefficient in (7) is generated

as $\psi_{k,l} = J_0(2\pi f_d T_s |k - l|)$ with $f_d = v f_c / c$ [34]–[36], where $J_0(\cdot)$ denotes the Bessel function of the first kind, $v = 30$ km/h denotes the velocity of the UT, $f_c = 30$ GHz denotes the carrier frequency, $c = 3 \times 10^8$ m/s denotes the speed of light, and $T_s = 0.5$ ms denotes the time interval between two adjacent synchronization time slots. The length of the synchronization signal \mathbf{X}_k is $L = 64$. We simulate total 500 drops to generate the arrival and departure angles $\theta_{r,p}$ and $\theta_{t,p}$ of each path in $[0, 1]$ randomly. In each drop, the arrival and departure angles are fixed, and only fast fading are considered. The total number of time slots is 10000 for each drop. The final performance curves are the average results of drops and time slots.

First, we consider the case with $K = 1$, i.e., the UT utilizes the received signal at $K = 1$ time slot to synchronize with the BS. This corresponds to the scenario with a short latency time and a relatively low success probability for initial synchronization. We compare the performance between three different precoding and combining approaches, including: 1) omnidirectional precoding and omnidirectional combining proposed in this paper; 2) quasi-omnidirectional precoding and omnidirectional combining; 3) random precoding and random combining. For Approach 1, we let $N_t^{(1)} = N_r^{(1)} = 2$. The precoding and combining matrices are generated according to (55) and (56), where $n_{t,k,1} = n_{r,k,1} = 1$, $n_{t,k,2} = M_t/2$, $n_{r,k,2} = M_r/2$, and $k = 1$ since $K = 1$. For Approach 2, we let $N_t^{(2)} = 1$ and $N_r^{(2)} = 2$. The precoding vector is set as a ZC sequence of length 64, and the combining matrix is the same as that in Approach 1. For Approach 3, we let $N_t^{(3)} = N_r^{(3)} = 1$. All the entries in the precoding and combining vectors have constant amplitudes and i.i.d. $\mathcal{U}(0, 2\pi)$ phases. To guarantee fair comparison, we let the FA probabilities of all these three approaches be equal to 10^{-4} . This can be achieved by letting $P_{\text{FA}} = 10^{-4}$ in (46) and then obtaining the corresponding threshold values $\gamma^{(1)}, \gamma^{(2)}, \gamma^{(3)}$ for these three approaches respectively.

The MD probabilities with respect to the SNR value for the above three approaches obtained from (24) are presented in Figs. 2 and 3. It can be observed that Approach 1, denoted as “omni precoding, omni combining”, has the best performance. This is because it can guarantee perfect omnidirectional coverage at both of the BS and UT sides, hence there is no transmission power fluctuation with respect to spatial angle directions. Since a ZC sequence is used as the precoding vector and random sequences are used as the precoding and combining vectors therein, Approaches 2 and 3, denoted as “omni combining, quasi-omni precoding” and “random combining, random precoding”, have transmission power nulls and fluctuation in spatial angle directions. This will lead to performance loss when the nulls or the angle directions with relatively

low power align with the channel paths. Moreover, for the case with $P = 4$ in Fig. 3, the performance curve of Approach 1 has a larger slope than the other two approaches. This is because the maximum achievable diversity order of Approach 1 is $N_r^{(1)}N_t^{(1)}K = 4$. When the actual channel has $P = 4$ paths, this diversity order can be exploited. Also note that the maximum achievable diversity orders of the other two approaches are $N_r^{(2)}N_t^{(2)}K = 2$ and $N_r^{(3)}N_t^{(3)}K = 1$, respectively. The relatively high SNR in Figs. 2 and 3 is because the UT needs to synchronize with the BS in a very short latency time ($KT = 0.5$ ms). This will obviously lead to poor synchronization performance. These two figures are mainly used to demonstrate that in the scenario with a short latency time and a relatively low success probability for initial synchronization, our proposed approach is superior to other existing approaches. In Figs. 4 and 5, where the latency time is relatively large ($KT = 32$ ms), the resulting SNR will be relatively low.

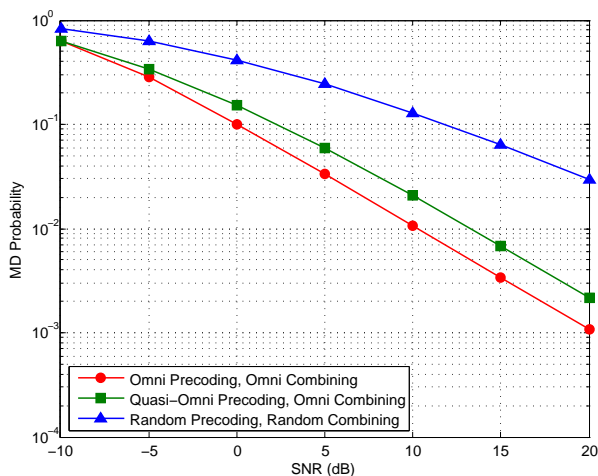


Fig. 2. Comparison of MD probability between different precoding and combining approaches, where $K = 1$ and $P = 1$.

Then, we consider the case with $K = 64$, i.e., the UT utilizes the received signals at $K = 64$ time slots to synchronize with the BS. This corresponds to the scenario with a long latency time and a relatively high success probability of initial synchronization. We compare the performance between three different precoding and combining approaches, including: 1) omnidirectional precoding and omnidirectional combining proposed in this paper; 2) beam-sweeping precoding and omnidirectional combining; 3) random precoding and random combining. For Approach 1, we let $N_t^{(1)} = N_r^{(1)} = 2$, and the precoding and combining matrices are generated according to (55) and (56), where $n_{t,k,1} = \binom{k}{M_t/2}$, $n_{t,k,2} = \binom{k}{M_t/2} + M_t/2$, $n_{r,k,1} = \binom{k}{M_r/2}$,

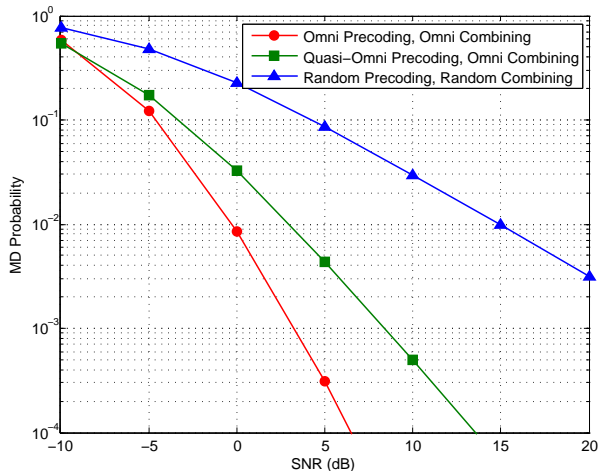


Fig. 3. Comparison of MD probability between different precoding and combining approaches, where $K = 1$ and $P = 4$.

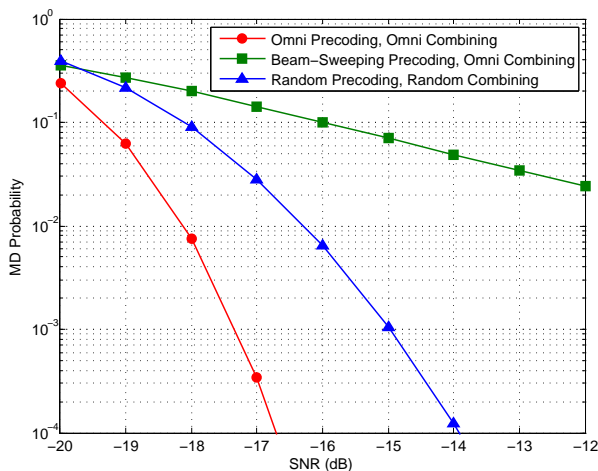


Fig. 4. Comparison of MD probability between different precoding and combining approaches, where $K = 64$ and $P = 1$.

$n_{r,k,2} = \binom{k}{M_r/2} + M_r/2$, and $k = 1, 2, \dots, 64$ since $K = 64$. For Approach 2, we let $N_t^{(2)} = 1$ and $N_r^{(2)} = 2$. The combining matrix is the same with that in Approach 1, and the precoding vector is set as the columns of a 64×64 discrete Fourier transform (DFT) matrix, i.e., $\frac{1}{\sqrt{64}}[1, e^{j2\pi k/64}, \dots, e^{j2\pi 63k/64}]^T$ for $k = 1, 2, \dots, 64$. For Approach 3, we let $N_t^{(3)} = N_r^{(3)} = 1$, and all the entries in the precoding and combining vectors at each time slot have constant amplitudes and i.i.d. $\mathcal{U}(0, 2\pi)$ phases. The FA probabilities of all these three approaches are set as 10^{-4} .

The MD probabilities with respect to the SNR value for the above three approaches obtained

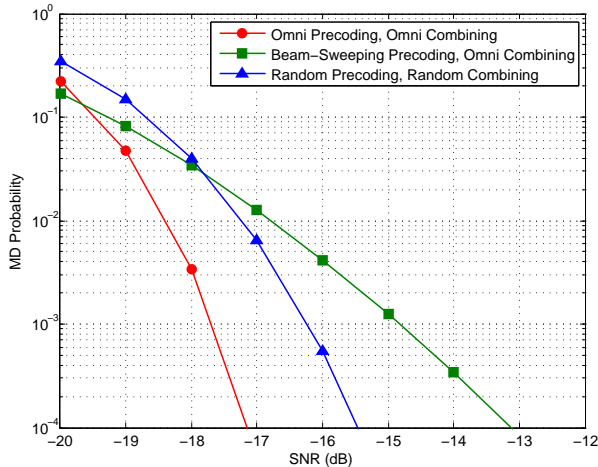


Fig. 5. Comparison of MD probability between different precoding and combining approaches, where $K = 64$ and $P = 4$.

from (24) are presented in Figs. 4 and 5. In Fig. 4, where the number of channel paths is $P = 1$, it can be observed that Approach 2, denoted as “beam-sweeping precoding, omni combining”, has a very poor performance. This is because it use narrow beams towards different spatial angle directions in total $K = 64$ time slots to guarantee omnidirectional coverage at the BS side. When there is only 1 channel path, the narrow beam could align with this path only at one time slot. At the other $K - 1 = 63$ time slots, the UT will receive little signal power. This implies that the effective channel between the BS and UT over the total $K = 64$ time slots will include 1 very strong component and 63 nearly zero components. Hence its time diversity order is only 1. As a comparison, Approach 1, denoted as “omni precoding, omni combining”, can guarantee omnidirectional coverage at every time slot. Therefore, the effective channel over the total $K = 64$ time slots will include 64 weak components, and time diversity order 64 can be exploited. In addition, for Approach 3, denoted as “random precoding, random combining”, the random precoding and combining vectors therein generate neither a perfect omnidirectional beam as Approach 1, nor a single narrow beam as Approach 2. Its performance is between those of Approaches 1 and 2. In Fig. 5, where the number of channel paths is $P = 4$, it can be observed that Approach 2 shows a better performance (larger slope) than that in Fig. 4. This is because when there are $P = 4$ paths having different spatial angles, the narrow beam could probably align with one of these 4 paths at 4 time slots. Therefore, the effective channel between the BS and UT over the total $K = 64$ time slots will include 4 relatively strong components and 60 nearly zero components. Hence time diversity order 4 can be obtained. Moreover, it has

to be noted that in Section IV-B when we analyze the effect of the precoding and combining matrices to the MD probability, we use the asymptotic MD probability (29) obtained at relatively high SNR (low MD probability) regime. This means that our proposed Approach 1 is preferable when the MD probability is low. In Fig. 5, we notice that when the SNR value is -20 dB, i.e., the MD probability is high (greater than 10^{-1}), the performance of Approach 2 is better than that of Approach 1. However, in practice, the MD probability should be low enough. Otherwise the synchronization may fail and the communication system may not work. Therefore, the low MD probability regime is relevant to practical applications, and our proposed Approach 1 shows significant performance gain in this regime.

VII. CONCLUSIONS

We have proposed an omnidirectional precoding and omnidirectional combining approach for mmWave massive MIMO synchronization. We demonstrated two basic requirements for the precoding and combining matrices, including that all the entries therein should have constant amplitude, and the transmission power averaged over the total K time slots should be constant for any spatial direction. Then, by utilizing the GLRT based synchronization detector, we analyzed the effect of the precoding and combining matrices to the MD probability and the FA probability, respectively, and present the corresponding conditions that should be satisfied. It is shown that, both of the precoding and combining matrices should guarantee perfectly omnidirectional coverage at each time slot, to minimize the asymptotic MD probability under the single-path channel. Since such omnidirectional precoding matrices and omnidirectional combining matrices exist only when both of the number of transmit streams and the number of receive streams are equal to or greater than two, we utilized Golay complementary pairs and Golay-Hadamard matrices to design the precoding and combining matrices. Simulation results verify the effectiveness of the propose approach.

APPENDIX A
PROOF OF THEOREM 1

With (1) and under hypothesis \mathcal{H}_1 , the logarithm of the probability density function (PDF) of the observed signal over K synchronization time slots can be expressed as

$$\begin{aligned} \ln f(\mathbf{Y}(\tau)|\mathcal{H}_1, \mathbf{G}, \nu) &= -KLN_r \ln(\pi\nu) - L \sum_{k=1}^K \ln \det(\mathbf{F}_k^H \mathbf{F}_k) \\ &\quad - \frac{1}{\nu} \sum_{k=1}^K \text{tr}((\mathbf{Y}_k(\tau) - \mathbf{G}_k \mathbf{X}_k)(\mathbf{Y}_k(\tau) - \mathbf{G}_k \mathbf{X}_k)^H (\mathbf{F}_k^H \mathbf{F}_k)^{-1}) \end{aligned} \quad (57)$$

where $\mathbf{Y}(\tau) = [\mathbf{Y}_1(\tau), \mathbf{Y}_2(\tau), \dots, \mathbf{Y}_K(\tau)]$ and $\mathbf{G} = [\mathbf{G}_1, \mathbf{G}_2, \dots, \mathbf{G}_K]$. It is easy to show that

$$\begin{aligned} \max_{\mathbf{G}, \nu} \ln f(\mathbf{Y}(\tau)|\mathcal{H}_1, \mathbf{G}, \nu) &= -L \sum_{k=1}^K \ln \det(\mathbf{F}_k^H \mathbf{F}_k) - KLN_r \\ &\quad - KLN_r \ln \left(\frac{\pi}{KLN_r} \sum_{k=1}^K \text{tr}((\mathbf{Y}_k(\tau) \mathbf{Y}_k^H(\tau) - \mathbf{Y}_k(\tau) \mathbf{X}_k^H (\mathbf{X}_k \mathbf{X}_k^H)^{-1} \mathbf{X}_k \mathbf{Y}_k^H(\tau)) (\mathbf{F}_k^H \mathbf{F}_k)^{-1}) \right). \end{aligned} \quad (58)$$

Similarly, under hypothesis \mathcal{H}_0 , we can have

$$\begin{aligned} \max_{\nu} \ln f(\mathbf{Y}(\tau)|\mathcal{H}_0, \nu) &= -L \sum_{k=1}^K \ln \det(\mathbf{F}_k^H \mathbf{F}_k) - KLN_r \\ &\quad - KLN_r \ln \left(\frac{\pi}{KLN_r} \sum_{k=1}^K \text{tr}(\mathbf{Y}_k(\tau) \mathbf{Y}_k^H(\tau) (\mathbf{F}_k^H \mathbf{F}_k)^{-1}) \right). \end{aligned} \quad (59)$$

Finally, with (58) and (59), we can express (18) as

$$\begin{aligned} T'(\tau) &= \max_{\mathbf{G}, \nu} \ln f(\mathbf{Y}(\tau)|\mathcal{H}_1, \mathbf{G}, \nu) - \max_{\nu} \ln f(\mathbf{Y}(\tau)|\mathcal{H}_0, \nu) \\ &= -KLN_r \ln \left(1 - \frac{\sum_{k=1}^K \text{tr}(\mathbf{Y}_k(\tau) \mathbf{X}_k^H (\mathbf{X}_k \mathbf{X}_k^H)^{-1} \mathbf{X}_k \mathbf{Y}_k^H(\tau) (\mathbf{F}_k^H \mathbf{F}_k)^{-1})}{\sum_{k=1}^K \text{tr}(\mathbf{Y}_k(\tau) \mathbf{Y}_k^H(\tau) (\mathbf{F}_k^H \mathbf{F}_k)^{-1})} \right) \stackrel{\mathcal{H}_1}{\geq} \stackrel{\mathcal{H}_0}{\gamma'}, \end{aligned}$$

and it is equivalent to (19) with variable substitution $\gamma = 1 - \exp\left(-\frac{\gamma'}{KLN_r}\right)$.

APPENDIX B
PROOF OF THEOREM 2 AND 3

First, we derive the probability of MD. Note that although we assume \mathbf{X}_k is unitary in (2), the derivation below can also be applied to the more general non-unitary case. Define the following matrix

$$\tilde{\mathbf{X}}_k = (\mathbf{X}_k \mathbf{X}_k^H)^{-1/2} \mathbf{X}_k. \quad (60)$$

It can be verified that $\tilde{\mathbf{X}}_k \in \mathbb{C}^{N_t \times L}$ satisfies

$$\tilde{\mathbf{X}}_k \tilde{\mathbf{X}}_k^H = (\mathbf{X}_k \mathbf{X}_k^H)^{-1/2} \mathbf{X}_k \mathbf{X}_k^H (\mathbf{X}_k \mathbf{X}_k^H)^{-1/2} = \mathbf{I}_{N_t}. \quad (61)$$

Then define another matrix $\tilde{\mathbf{X}}_k^\perp \in \mathbb{C}^{(L-N_t) \times L}$ satisfying

$$\begin{bmatrix} \tilde{\mathbf{X}}_k^\perp \\ \tilde{\mathbf{X}}_k \end{bmatrix} \begin{bmatrix} \tilde{\mathbf{X}}_k^\perp \\ \tilde{\mathbf{X}}_k \end{bmatrix}^H = \begin{bmatrix} \mathbf{I}_{L-N_t} & \mathbf{0} \\ \mathbf{0} & \mathbf{I}_{N_t} \end{bmatrix} = \mathbf{I}_L, \quad (62)$$

i.e., $\tilde{\mathbf{X}}_k^\perp$ and $\tilde{\mathbf{X}}_k$ constitute an $L \times L$ unitary matrix. With the property of unitary matrices, we can also write (62) as

$$\begin{bmatrix} \tilde{\mathbf{X}}_k^\perp \\ \tilde{\mathbf{X}}_k \end{bmatrix}^H \begin{bmatrix} \tilde{\mathbf{X}}_k^\perp \\ \tilde{\mathbf{X}}_k \end{bmatrix} = \mathbf{I}_L. \quad (63)$$

With (1) and under hypothesis \mathcal{H}_1 , we have

$$(\mathbf{F}_k^H \mathbf{F}_k)^{-1/2} \mathbf{Y}_k(\tau) = (\mathbf{F}_k^H \mathbf{F}_k)^{-1/2} (\mathbf{G}_k \mathbf{X}_k + \mathbf{F}_k^H \mathbf{Z}_k) = \tilde{\mathbf{G}}_k \tilde{\mathbf{X}}_k + \tilde{\mathbf{Z}}_k \quad (64)$$

where the last equality is from (60), and

$$\tilde{\mathbf{G}}_k = (\mathbf{F}_k^H \mathbf{F}_k)^{-1/2} \mathbf{G}_k (\mathbf{X}_k \mathbf{X}_k^H)^{1/2} \quad (65)$$

$$\tilde{\mathbf{Z}}_k = (\mathbf{F}_k^H \mathbf{F}_k)^{-1/2} \mathbf{F}_k^H \mathbf{Z}_k. \quad (66)$$

Since \mathbf{Z}_k is with i.i.d. $\mathcal{CN}(0, \nu)$ entries, $\tilde{\mathbf{Z}}_k$ in (66) is also with i.i.d. $\mathcal{CN}(0, \nu)$ entries. Then we have

$$\begin{aligned} (\mathbf{F}_k^H \mathbf{F}_k)^{-1/2} \mathbf{Y}_k(\tau) \mathbf{Y}_k^H(\tau) (\mathbf{F}_k^H \mathbf{F}_k)^{-1/2} &= (\tilde{\mathbf{G}}_k \tilde{\mathbf{X}}_k + \tilde{\mathbf{Z}}_k) \begin{bmatrix} \tilde{\mathbf{X}}_k^\perp \\ \tilde{\mathbf{X}}_k \end{bmatrix}^H \begin{bmatrix} \tilde{\mathbf{X}}_k^\perp \\ \tilde{\mathbf{X}}_k \end{bmatrix} (\tilde{\mathbf{G}}_k \tilde{\mathbf{X}}_k + \tilde{\mathbf{Z}}_k)^H \\ &= [\tilde{\mathbf{Z}}_k \tilde{\mathbf{X}}_k^{\perp H}, \tilde{\mathbf{G}}_k + \tilde{\mathbf{Z}}_k \tilde{\mathbf{X}}_k^H] [\tilde{\mathbf{Z}}_k \tilde{\mathbf{X}}_k^{\perp H}, \tilde{\mathbf{G}}_k + \tilde{\mathbf{Z}}_k \tilde{\mathbf{X}}_k^H]^H = \mathbf{Z}_{k,1} \mathbf{Z}_{k,1}^H + (\tilde{\mathbf{G}}_k + \mathbf{Z}_{k,2})(\tilde{\mathbf{G}}_k + \mathbf{Z}_{k,2})^H \end{aligned} \quad (67)$$

where the first equality is from (64) and (63), the second equality is from (62), $\mathbf{Z}_{k,1} = \tilde{\mathbf{Z}}_k \tilde{\mathbf{X}}_k^{\perp H} \in \mathbb{C}^{N_r \times (L-N_t)}$ and $\mathbf{Z}_{k,2} = \tilde{\mathbf{Z}}_k \tilde{\mathbf{X}}_k^H \in \mathbb{C}^{N_r \times N_t}$ are both with i.i.d. $\mathcal{CN}(0, \nu)$ entries. In addition, we have

$$\begin{aligned} (\mathbf{F}_k^H \mathbf{F}_k)^{-1/2} \mathbf{Y}_k(\tau) \mathbf{X}_k^H (\mathbf{X}_k \mathbf{X}_k^H)^{-1} \mathbf{X}_k \mathbf{Y}_k^H(\tau) (\mathbf{F}_k^H \mathbf{F}_k)^{-1/2} \\ = (\tilde{\mathbf{G}}_k \tilde{\mathbf{X}}_k + \tilde{\mathbf{Z}}_k) \tilde{\mathbf{X}}_k^H \tilde{\mathbf{X}}_k (\tilde{\mathbf{G}}_k \tilde{\mathbf{X}}_k + \tilde{\mathbf{Z}}_k)^H = (\tilde{\mathbf{G}}_k + \mathbf{Z}_{k,2})(\tilde{\mathbf{G}}_k + \mathbf{Z}_{k,2})^H \end{aligned} \quad (68)$$

where the first equality is from (64) and (60), and the last equality is from (61). Therefore, with (68) and (67), the test statistic T in (19) under hypothesis \mathcal{H}_1 can be expressed as

$$\begin{aligned} T(\tau)|\mathcal{H}_1 &= \frac{\sum_{k=1}^K \text{tr}((\tilde{\mathbf{G}}_k + \mathbf{Z}_{k,2})(\tilde{\mathbf{G}}_k + \mathbf{Z}_{k,2})^H)}{\sum_{k=1}^K \text{tr}(\mathbf{Z}_{k,1}\mathbf{Z}_{k,1}^H + (\tilde{\mathbf{G}}_k + \mathbf{Z}_{k,2})(\tilde{\mathbf{G}}_k + \mathbf{Z}_{k,2})^H)} \\ &= \frac{\sum_{k=1}^K \|(L/N_t)^{1/2}(\mathbf{F}_k^H \mathbf{F}_k)^{-1/2} \mathbf{F}_k^H \mathbf{H}_k \mathbf{W}_k + \mathbf{Z}_{k,2}\|_{\mathbb{F}}^2}{\sum_{k=1}^K (\|\mathbf{Z}_{k,1}\|_{\mathbb{F}}^2 + \|(L/N_t)^{1/2}(\mathbf{F}_k^H \mathbf{F}_k)^{-1/2} \mathbf{F}_k^H \mathbf{H}_k \mathbf{W}_k + \mathbf{Z}_{k,2}\|_{\mathbb{F}}^2)} \end{aligned} \quad (69)$$

where the last equality is with (65) and (2). Note that in (69) it always holds that $(\mathbf{F}_k^H \mathbf{F}_k)^{-1/2} \mathbf{F}_k^H \cdot \mathbf{F}_k (\mathbf{F}_k^H \mathbf{F}_k)^{-1/2} = \mathbf{I}_{N_r}$ for any \mathbf{F}_k with full column rank. Hence we can rewrite (69) as

$$T(\tau)|\mathcal{H}_1 = \frac{\sum_{k=1}^K \|(L/N_t)^{1/2} \mathbf{F}_k^H \mathbf{H}_k \mathbf{W}_k + \mathbf{Z}_{k,2}\|_{\mathbb{F}}^2}{\sum_{k=1}^K (\|\mathbf{Z}_{k,1}\|_{\mathbb{F}}^2 + \|(L/N_t)^{1/2} \mathbf{F}_k^H \mathbf{H}_k \mathbf{W}_k + \mathbf{Z}_{k,2}\|_{\mathbb{F}}^2)} \quad (70)$$

for notational simplicity, where \mathbf{F}_k satisfies $\mathbf{F}_k^H \mathbf{F}_k = \mathbf{I}_{N_r}$. Since $T < \gamma$ is equivalent to $\frac{T}{1-T} < \frac{\gamma}{1-\gamma}$, the MD probability (20) can be expressed as (22) according to (70).

To derive the FA probability, we can let $\mathbf{H}_k = \mathbf{0}$ in (70), yielding the test statistic T under hypothesis \mathcal{H}_0

$$T|\mathcal{H}_0 = \frac{\sum_{k=1}^K \|\mathbf{Z}_{k,2}\|_{\mathbb{F}}^2}{\sum_{k=1}^K (\|\mathbf{Z}_{k,1}\|_{\mathbb{F}}^2 + \|\mathbf{Z}_{k,2}\|_{\mathbb{F}}^2)}.$$

Therefore, the FA probability (21) can be expressed as (45).

APPENDIX C

PROOF OF LEMMA 1

First, we derive the characteristic function (CF) and the n th non-central moment of X , which will be used latter. For $x_m \sim \mathcal{CN}(0, \lambda_m)$, $X_m = |x_m|^2$ follows exponential distribution and the CF of X_m is

$$\varphi_{X_m}(\omega) = \mathbb{E}\{e^{-j\omega X_m}\} = \frac{1}{1 + j\lambda_m \omega}.$$

Then, the CF of $X = \sum_{m=1}^M X_m$ is

$$\varphi_X(\omega) = \mathbb{E}\{e^{-j\omega X}\} = \prod_{m=1}^M \varphi_{X_m}(\omega) = \prod_{m=1}^M \frac{1}{1 + j\lambda_m \omega}. \quad (71)$$

Let $f_X(x)$ denote the PDF of X . According to the relation between CF and PDF

$$\varphi_X(\omega) = \int_0^{\infty} f_X(x) e^{-j\omega x} dx, \quad (72)$$

we have

$$\frac{d^n \varphi_X(\omega)}{d\omega^n} = (-j)^n \int_0^\infty x^n f_X(x) e^{-j\omega x} dx.$$

Therefore,

$$\mathbb{E}\{X^n\} = \int_0^\infty x^n f_X(x) dx = (-j)^{-n} \frac{d^n \varphi_X(\omega)}{d\omega^n} \Big|_{\omega=0}. \quad (73)$$

With the general Leibniz rule, the n th derivative of $\varphi_X(\omega)$ is

$$\begin{aligned} \frac{d^n \varphi_X(\omega)}{d\omega^n} &= \frac{d^n}{d\omega^n} \left(\prod_{m=1}^M \frac{1}{1 + j\lambda_m \omega} \right) \\ &= \sum_{k_1+k_2+\dots+k_M=n} \binom{n}{k_1, k_2, \dots, k_M} \prod_{m=1}^M \frac{d^{k_m}}{d\omega^{k_m}} \left(\frac{1}{1 + j\lambda_m \omega} \right) \\ &= \sum_{k_1+k_2+\dots+k_M=n} \frac{n!}{k_1! k_2! \dots k_M!} \prod_{m=1}^M \frac{(-j\lambda_m)^{k_m} k_m!}{(1 + j\lambda_m \omega)^{k_m+1}} \\ &= (-j)^n n! \sum_{k_1+k_2+\dots+k_M=n} \prod_{m=1}^M \frac{\lambda_m^{k_m}}{(1 + j\lambda_m \omega)^{k_m+1}} \end{aligned} \quad (74)$$

where each k_m is a non-negative integer. Substituting (74) into (73) yields

$$\mathbb{E}\{X^n\} = n! \sum_{k_1+k_2+\dots+k_M=n} \prod_{m=1}^M \lambda_m^{k_m}. \quad (75)$$

Then, we derive the asymptotic value for the CDF of X/Y . Since X and Y are independent with each other, we have

$$\mathbb{P}\left\{\frac{X}{Y} < t\right\} = \mathbb{P}\{X < tY\} = \int_0^\infty f_Y(y) \int_0^{ty} f_X(x) dx dy. \quad (76)$$

To derive the asymptotic value of (76) when t is small, we use (71) to obtain the Taylor series expansion of $\varphi_X(\omega)$ at $1/(j\omega) = 0$

$$\varphi_X(\omega) = \frac{1}{(j\omega)^M} \prod_{m=1}^M \frac{1}{1/j\omega + \lambda_m} = \frac{1}{(j\omega)^M} \sum_{k=0}^{\infty} \frac{a_k}{(j\omega)^k}$$

where

$$a_k = \sum_{k_1+k_2+\dots+k_M=k} \frac{1}{k_1! k_2! \dots k_M!} \prod_{m=1}^M \frac{(-1)^{k_m}}{\lambda_m^{k_m+1}}. \quad (77)$$

Then the PDF of X is

$$f_X(x) = \frac{1}{2\pi} \int_{-\infty}^{\infty} \varphi_X(\omega) e^{j\omega x} d\omega = \frac{1}{2\pi} \int_{-\infty}^{\infty} \frac{1}{(j\omega)^M} \sum_{k=0}^{\infty} \frac{a_k}{(j\omega)^k} e^{j\omega x} d\omega = u(x) \cdot \sum_{k=0}^{\infty} \frac{a_k x^{M+k-1}}{(M+k-1)!}$$

where $u(x)$ denotes the unit step function, i.e., $u(x) = 1$ when $x \geq 0$ and $u(x) = 0$ when $x < 0$.

Then we have

$$\int_{-\infty}^{ty} f_X(x) dx = \int_0^{ty} \sum_{k=0}^{\infty} \frac{a_k x^{M+k-1}}{(M+k-1)!} dx = \sum_{k=0}^{\infty} \frac{a_k (ty)^{M+k}}{(M+k)!}$$

and hence

$$\begin{aligned} \mathbb{P}\left\{\frac{X}{Y} < t\right\} &= \int_0^{\infty} f_Y(y) \int_0^{ty} \sum_{k=0}^{\infty} \frac{a_k x^{M+k-1}}{(M+k-1)!} dx dy = \int_{-\infty}^{\infty} f_Y(y) \sum_{k=0}^{\infty} \frac{a_k (ty)^{M+k}}{(M+k)!} dy \\ &= \sum_{k=0}^{\infty} \frac{a_k t^{M+k} \mathbb{E}\{y^{M+k}\}}{(M+k)!} = \sum_{k=0}^{\infty} a_k t^{M+k} \sum_{l_1+l_2+\dots+l_N=M+k} \prod_{n=1}^N \sigma_n^{l_n} \\ &\approx a_0 t^M \sum_{l_1+l_2+\dots+l_N=M} \prod_{n=1}^N \sigma_n^{l_n}, \quad \text{when } t \text{ is small,} \end{aligned} \quad (78)$$

where the last equality is with (75). Substituting (77) with $k = 0$ into (78) yields (28).

REFERENCES

- [1] Z. Pi and F. Khan, "An introduction to millimeter-wave mobile broadband systems," *IEEE Commun. Mag.*, vol. 49, no. 6, pp. 101–107, Jun. 2011.
- [2] T. S. Rappaport et al., "Millimeter wave mobile communications for 5G cellular: It will work!" *IEEE Access*, vol. 1, pp. 335–349, May 2013.
- [3] M. R. Akdeniz, Y. Liu, M. K. Samimi, S. Sun, S. Rangan, T. S. Rappaport, and E. Erkip, "Millimeter wave channel modeling and cellular capacity evaluation," *IEEE J. Sel. Areas Commun.*, vol. 32, no. 6, pp. 1164–1179, Jun. 2014.
- [4] W. Roh et al., "Millimeter-wave beamforming as an enabling technology for 5G cellular communications: Theoretical feasibility and prototype results," *IEEE Commun. Mag.*, vol. 52, no. 2, pp. 106–113, Feb. 2014.
- [5] T. Bai and R. W. Heath, "Coverage and rate analysis for millimeter-wave cellular networks," *IEEE Trans. Wireless Commun.*, vol. 14, no. 2, pp. 1100–1114, Feb. 2015.
- [6] X. Yang, W. Jiang, and B. Vucetic, "A random beamforming technique for omnidirectional coverage in multiple-antenna systems," *IEEE Trans. Veh. Technol.*, vol. 62, no. 3, pp. 1420–1425, Mar. 2013.
- [7] T. S. Rappaport, R. W. Heath, R. C. Daniels, and J. N. Murdock, *Millimeter Wave Wireless Communications*, Englewood Cliffs, NJ, USA: Prentice-Hall, 2015.
- [8] Q. Li, H. Niu, G. Wu, and R. Q. Hu, "Anchor-booster based heterogeneous networks with mmwave capable booster cells," in *Proc. IEEE GLOBECOM Workshops*, Atlanta, GA, USA, Dec. 2013, pp. 93–98.
- [9] S. Sesia, I. Toufik, and M. Baker, *LTE – The UMTS Long Term Evolution: From Theory to Practice*. John Wiley & Sons, 2009.
- [10] C. N. Barati, S. A. Hosseini, S. Rangan, P. Liu, T. Korakis, S. S. Panwar, and T. S. Rappaport, "Directional cell discovery in millimeter wave cellular networks," *IEEE Trans. Wireless Commun.*, vol. 14, no. 12, pp. 6664–6678, Dec. 2015.
- [11] C. N. Barati, S. A. Hosseini, M. Mezzavilla, T. Korakis, S. S. Panwar, S. Rangan, and M. Zorzi, "Initial access in millimeter wave cellular systems," *IEEE Trans. Wireless Commun.*, vol. 15, no. 12, pp. 7926–7940, Dec. 2016.
- [12] C. Liu, M. Li, I. B. Collings, S. V. Hanly, and P. Whiting, "Design and analysis of transmit beamforming for millimetre wave base station discovery," *IEEE Trans. Wireless Commun.*, vol. 16, no. 2, pp. 797–811, Feb. 2017.

- [13] V. Raghavan, J. Cezanne, S. Subramanian, A. Sampath, and O. Koymen, “Beamforming tradeoffs for initial UE discovery in millimeter-wave MIMO systems,” *IEEE J. Sel. Topics Signal Process.*, vol. 10, no. 3, pp. 543–559, Apr. 2016.
- [14] L. You, X. Q. Gao, G. Y. Li, X.-G. Xia, and N. Ma, “BDMA for millimeter-wave/terahertz massive MIMO transmission with per-beam synchronization,” *IEEE J. Sel. Areas Commun.*, vol. 35, no. 7, pp. 1550–1563, Jul. 2017.
- [15] S. M. Kay, *Fundamentals of Statistical Signal Processing*. Upper Saddle River, NJ, USA: Prentice-Hall, 1998.
- [16] D. W. Bliss and P. A. Parker, “Temporal synchronization of MIMO wireless communication in the presence of interference,” *IEEE Trans. Signal Process.*, vol. 58, no. 3, pp. 1794–1806, Mar. 2010.
- [17] A. M. Sayeed, “Deconstructing multi-antenna fading channels,” *IEEE Trans. Signal Process.*, vol. 50, no. 10, pp. 2563–2579, Oct. 2002.
- [18] D. Tse and P. Viswanath, *Fundamentals of Wireless Communication*. Cambridge, UK: Cambridge Univ. Press, 2005.
- [19] Y. Wang, L. Huang, Z. Shi, K. Liu, and X. Zou, “A millimeter wave channel model with variant angles under 3GPP SCM framework,” in *Proc. IEEE PIMRC*, Hongkong, China, Aug.–Sept. 2015, pp. 2249–2254.
- [20] I. Viering, H. Hofstetter, and W. Utschick, “Validity of spatial covariance matrices over time and frequency,” in *Proc. IEEE GLOBECOM*, Taipei, Taiwan, Nov. 2002, pp. 851–855.
- [21] M. Nicoli, O. Simeone, and U. Spagnolini, “Multislot estimation of fast-varying space-time communication channels,” *IEEE Trans. Signal Process.*, vol. 51, no. 5, pp. 1184–1195, May 2003.
- [22] A. Alkhateeb, J. Mo, N. Gonzalez-Prelcic, and R. W. Heath, “MIMO precoding and combining solutions for millimeter-wave systems,” *IEEE Commun. Mag.*, vol. 52, no. 12, pp. 122–131, Dec. 2014.
- [23] S. Han, C.-L. I, Z. Xu, and C. Rowell, “Large-scale antenna systems with hybrid analog and digital beamforming for millimeter wave 5G,” *IEEE Commun. Mag.*, vol. 53, no. 1, pp. 186–194, Jan. 2015.
- [24] O. E. Ayach, S. Rajagopal, S. Abu-Surra, Z. Pi, and R. W. Heath, “Spatially sparse precoding in millimeter wave MIMO systems,” *IEEE Trans. Wireless Commun.*, vol. 13, no. 3, pp. 1499–1513, Mar. 2014.
- [25] V. Tarokh, N. Seshadri, and A. R. Calderbank, “Space-time codes for high data rate wireless communication: Performance criterion and code construction,” *IEEE Trans. Inf. Theory*, vol. 44, no. 2, pp. 744–765, Mar. 1998.
- [26] C. Walck, *Handbook on Statistical Distributions for Experimentalists*. Stockholm, Sweden: Univ. Stockholm Press, 2007.
- [27] X. Meng, X. Q. Gao, and X.-G. Xia, “Omnidirectional precoding based transmission in massive MIMO systems,” *IEEE Trans. Commun.*, vol. 64, no. 1, pp. 174–186, Jan. 2016.
- [28] X. Meng, X.-G. Xia, and X. Q. Gao, “Omnidirectional space-time block coding for common information broadcasting in massive MIMO systems,” *IEEE Trans. Wireless Commun.*, DOI: 10.1109/TWC.2016.2622259.
- [29] M. J. E. Golay, “Multi-slit spectrometry,” *J. Opt. Soc. Amer.*, vol. 39, no. 6, pp. 437–444, Jun. 1949.
- [30] M. J. E. Golay, “Complementary series,” *IRE Trans. Inf. Theory*, vol. 7, no. 2, pp. 82–87, Apr. 1961.
- [31] M. J. E. Golay, “Seives for low autocorrelation binary sequences,” *IEEE Trans. Inf. Theory*, vol. 23, no.1 pp. 43–51, Jan. 1977.
- [32] J. A. Davis and J. Jedwab, “Peak-to-mean power control in OFDM, Golay complementary sequences and Reed-Muller codes,” *IEEE Trans. Inf. Theory*, vol. 45, no. 7, pp. 2397–2417, Nov. 1999.
- [33] X. Huang and Y. Li, “Scalable complete complementary sets of sequences,” in *Proc. IEEE GLOBECOM*, Taipei, Taiwan, Nov. 2002, pp. 1056–1060.
- [34] J. Choi, D. J. Love, and P. Bidigare, “Downlink training techniques for FDD massive MIMO systems: Open-loop and closed-loop training with memory,” *IEEE J. Sel. Topics Signal Process.*, vol. 8, no. 5, pp. 802–814, Oct. 2014.
- [35] J. He, T. Kim, H. Ghanch, K. Liu, and G. Wang, “Millimeter wave MIMO channel tracking systems,” in *Proc. IEEE GLOBECOM Workshops*, Austin, TX, USA, Dec. 2014, pp. 416–421.

- [36] G. C. Alexandropoulos and S. Chouvardas, "Low complexity channel estimation for millimeter wave systems with hybrid A/D antenna processing," in *Proc. IEEE GLOBECOM Workshops*, Washington, DC, USA, Dec. 2016.